(4)

GL-TR-89-0102

AD-A209 254

Lg-Wave Propagation in Heterogeneous Media

Brian L. N. Kennett

Australian National University
Research School of Earth Sciences
GPO Box 4
Canberra ACT 2601
AUSTRALIA

DTIC
S ELECTE
JUN 2 1 1989
D D

6 April 1989

Final Report
15 February 1988–14 February 1989

GEOPHYSICS LABORATORY
AIR FORCE SYSTEMS COMMAND
UNITED STATES AIR FORCE
HANSCOM AIR FORCE BASE, MASSACHUSETTS 01731-5000

89   6   20   241

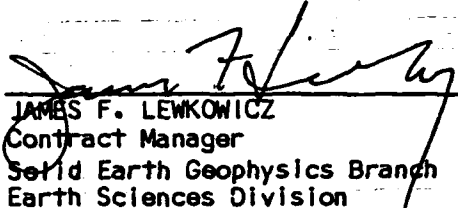The views and conclusions contained in this document are those of the authors and should not be interpreted as representing the official policies, either expressed or implied, of the Defense Advanced Research Projects Agency or the U.S. Government.

This technical report has been reviewed and is approved for publication.

JAMES F. LEWKOWICZ
Contract Manager
Solid Earth Geophysics Branch
Earth Sciences Division

JAMES F. LEWKOWICZ
Branch Chief
Solid Earth Geophysics Branch
Earth Sciences Division

FOR THE COMMANDER

DONALD H. ECKHARDT, Director
Earth Sciences Division

This report has been reviewed by the ESD Public Affairs Office (PA) and is releasable to the National Technical Information Service (NTIS).

Qualified requestors may obtain additional copies from the Defense Technical Information Center. All others should apply to the National Technical Information Service.

If your address has changed, or if you wish to be removed from the mailing list, or if the addressee is no longer employed by your organization, please notify AFGL/DAA, Hanscom AFB, MA 01731-5000. This will assist us in maintaining a current mailing list.

Do not return copies of this report unless contractual obligations or notices on a specific document requires that it be returned.

REPORT DOCUMENTATION PAGE		Form Approved OMB No. 0704-0188

1a. REPORT SECURITY CLASSIFICATION UNCLASSIFIED	1b. RESTRICTIVE MARKINGS

2a. SECURITY CLASSIFICATION AUTHORITY	3. DISTRIBUTION / AVAILABILITY OF REPORT
2b. DECLASSIFICATION / DOWNGRADING SCHEDULE	Approved for Public Release Distribution Unlimited

4. PERFORMING ORGANIZATION REPORT NUMBER(S)	5. MONITORING ORGANIZATION REPORT NUMBER(S) GL-TR-89-0102

6a. NAME OF PERFORMING ORGANIZATION Research School of Earth Sciences	6b. OFFICE SYMBOL (If applicable)	7a. NAME OF MONITORING ORGANIZATION Geophysics Laboratory

6c. ADDRESS (City, State, and ZIP Code) Australian National University GPO Box 4, CANBERRA ACT 2601, Australia	7b. ADDRESS (City, State, and ZIP Code) Hanscom AFB Massachusetts 01731-5000

8a. NAME OF FUNDING / SPONSORING ORGANIZATION Geophysics Laboratory	8b. OFFICE SYMBOL (If applicable)	9. PROCUREMENT INSTRUMENT IDENTIFICATION NUMBER Grant AFOSR-87-0187

8c. ADDRESS (City, State, and ZIP Code) Hanscom AFB Masschusetts 01731-5000	10. SOURCE OF FUNDING NUMBERS			
	PROGRAM ELEMENT NO. 61101E	PROJECT NO. 7A10	TASK NO DA	WORK UNIT ACCESSION NO. CB

11. TITLE (Include Security Classification)

Lg-wave Propagation in Heterogeneous Media   (Unclassified)

12. PERSONAL AUTHOR(S)
KENNETT, Brian L.N.

13a. TYPE OF REPORT Final	13b. TIME COVERED FROM 88/2/15 TO 89/2/14	14. DATE OF REPORT (Year, Month, Day) 1989 April 6	15. PAGE COUNT 68

16. SUPPLEMENTARY NOTATION

17. COSATI CODES			18. SUBJECT TERMS (Continue on reverse if necessary and identify by block number)
FIELD	GROUP	SUB-GROUP	Wave propagation Lg waves Heterogeneity Coupled Modes Operator Methods

19. ABSTRACT (Continue on reverse if necessary and identify by block number)

The Lg wave is of importance for nuclear discrimination problems because it is commonly the largest phase on a seismic record at regional ranges. It is therefore likely to be detected even for quite small events. The energy comprising Lg is dominantly guided in the crustal waveguide which is known to be a region with very considerable horizontal variability in properties.

The effect of heterogeneity on Lg and other regional phases has been assessed by the development of a new method for the description of seismic wave propagation processes in laterally varying media. This scheme is based on propagation operators which allow for the major processes of interconversion between seismic wavetypes. This approach is used to generate descriptions of the propagation processes contributing to the main regional seismic phases Pn, Pg, Sn and Lg. These representations are

20. DISTRIBUTION / AVAILABILITY OF ABSTRACT ☐ UNCLASSIFIED/UNLIMITED ☒ SAME AS RPT. ☐ DTIC USERS	21. ABSTRACT SECURITY CLASSIFICATION Unclassified
22a. NAME OF RESPONSIBLE INDIVIDUAL James F. Lewkowicz	22b. TELEPHONE (Include Area Code) (617) 377-3028	22c. OFFICE SYMBOL LWH

DD Form 1473, JUN 86   *Previous editions are obsolete.*

19. ABSTRACT (continued)

then used to examine the theoretical basis for the discriminants between earthquakes and underground nuclear explosions based on the relative amplitudes of P and S waves. The ratio of Sn to Pn amplitude looks promising as a high frequency discriminant. However, the ratio of Lg to Pn amplitudes is not as useful because of the complex nature of the propagation characteristics of Lg. (; 4 d) ⊂

An implementation of the operator method by means of coupled modes has been used to examine the effect of heterogeneous crustal structures on Lg. In this technique the local seismic wavefield in the real medium is expressed as a combination of the modal eigenfunctions of a stratified reference structure. Departures of the seismic properties in the real medium from those in the reference lead to coupling between the amplitude coefficients in the modal expansion. The evolution of these modal weighting functions with horizontal position are described by a coupled set of ordinary differential equations. This approach provides a calculation scheme for studying guided wave propagation over extended distances, at frequencies of 1 Hz and above. The heterogeneity models which have been used are two-dimensional and calculations are carried out for one frequency at a time.

One of the major effects of crustal heterogeneity is to introduce the possibility of changing the character of the main amplitude peak in the Lg wavetrain by shifting energy between different group velocity components. As a result, an effective measure of the energy content of the Lg waves will be to consider the integrated energy along the trace between group velocities of 3.6 and 3.3 km/s. The effects of heterogeneity vary between different parts of the Lg wave train and can be visualised by using synthetic seismograms computed with a narrow band response in frequency, with allowance for interaction between the modes. The representation of the wavefield in terms of modal contributions allows a detailed analysis in terms of the group velocity components.

RESEARCH OBJECTIVES

The aim of this work is to develop techniques which can be used to describe the propagation of regional seismic phases in three-dimensionally heterogeneous media, in order to improve the understanding of the nature of the phases and the way in which'the characteristics of the seismic source can be modified by propagation to the receiver. Such information will be valuable in assessing the effects of geological structure on the behaviour of potential discriminants between earthquakes and underground nuclear explosions.

Most of the regional phases of interest for nuclear discrimination problems are observed after propagation through considerable distances. These phases travel through the crust and uppermost mantle, which from a wide variety of studies are known to be regions of considerable horizontal variability of properties.

We have therefore set out to find theoretical descriptions of the propagation of the regional phases which enable us to find general results on the relative amplitudes of different phases. In addition we have undertaken a computational study of the interaction of the Lg phase with specific models of heterogeneity

RESEARCH STATUS AND ACHIEVEMENTS

In general, observations of regional seismic phases are made at some hundreds of kilometres from the source, so that the waves can have made quite complex interactions with three-dimensional heterogeneity in the crust and uppermost mantle. The descriptions of the propagation process is a difficult mathematical task but can be simplified by introducing the concept of propagation operators (Kennett 1986). This approach allows the sequence of physical processes from the generation of the seismic waves at the source to reception at the sensors to be represented as the action of a set of operators on the up and downgoing waves generated at the source.

Useful approximations in the operator development to concentrate attention on the dominant modes of propagation can be made by exploiting analogies with earlier work on stratified media. The particular implementation for the operators can be adapted to suit the particular nature of the process being described.

This operator representation has been used to look at the theoretical characteristics of a variety of potential discriminants between earthquakes and underground nuclear explosions based on the ratio of P and S wave amplitudes.

A full description of the operator approach and the discrimination results are given in the attached paper: *On the nature of regional seismic phases I - phase representations for Pn, Pg, Sn and Lg.*

Many existing techniques for describing the propagation of guided waves
in heterogeneous media can be regarded as implementations of the operator
approach. The coupled mode technique of Kennett (1984) allows for
interactions with heterogeneity by allowing the transfer of energy between
different modes with different horizontal wave-numbers, thereby
redistributing the energy between different group velocity and so changing
the character of the seismic record. This approach is particularly suited
for examining the effect of modest heterogeneity on regional S wavetrains
which can be described by a limited number of discrete modes.

In the accompanying paper: *Lg wave propagation in heterogeneous media*,
a sequence of models with varying levels of heterogeneity have been used
to determine the merits and limitations of the coupled mode computation
scheme. The technique works well with heterogeneous models in which the
local seismic velocities differ from the stratified reference by up to
2 per cent without significant perturbation of the major interfaces (such
as the crust-mantle boundary). Localised changes in seismic velocities
and density can be even larger, but it is difficult to account for shifts
of more than 2-3 km in the position of the Moho.

The nature of the modifications produced by Lg propagation through with
heterogeneity can be clearly seen by constructing theoretical seismograms
with a narrow frequency band and then incorporating the inter-mode
coupling. The shape of the main amplitude maximum is modified and there
can be transfer of energy to Sn which tends to extend the duration of
significant signal.

REFERENCES

Kennett B.L.N. (1984) Guided wave propagation in laterally varying media -
    I. Theoretical development, *Geophys. J. R. astr. Soc.*, **79**, 235-255

Kennett B.L.N. (1986) Wavenumber and wavetype coupling in laterally
    heterogeneous media, *Geophys. J. R. astr. Soc.*, **87**, 313-331

On the nature of regional seismic phases I
- phase representations for Pn, Pg, Sn, Lg

B.L.N. Kennett

Research School of Earth Sciences,
Australian National University,·
G.P.O. Box 4, Canberra, A.C.T. 2601
Australia

Summary

An operator development of the seismic wavefield is used to generate descriptions of the propagation processes contributing to the main regional seismic phases Pn, Pg, Sn, Lg. These operator forms are valid for laterally heterogeneous crust and mantle models and include the major processes of interconversion between wavetypes.

These representations of the regional phases are used to examine the theoretical basis for discriminants between earthquakes and underground explosions based on the relative amplitudes of P and S phases. The ratio of Sn to Pn amplitude looks promising as a high frequency discriminant. However, the ratio of Lg to Pn amplitudes is not as useful because of the complex nature of the propagation characteristics of Lg.

Key Words: regional phases, wave propagation, laterally
heterogeneous media, Pn, Pg, Sn, Lg, source discrimination

Introduction

The propagation of seismic phases at regional distances has been a topic of continuous interest since the work of Mohorovicic (1909) on the Kulpatal earthquake in Croatia, and these phases have been extensively used to determine the structure of the crust and uppermost mantle. These structural studies, especially for P waves, lead to the development of many analysis tools such as the computation of theoretical seismograms for realistic models (see e.g. Fuchs & Müller 1971). A major impetus to understand the detailed characteristics of the regional wavefield has come with efforts to monitor underground explosions of low yield and discriminate them from earthquakes (see e.g. Pomeroy et al 1982).

Despite this long term interest, there has been considerable debate about the nature of the propagation processes giving rise to the most prominent of the observed regional phases Pn, Pg, Sn, Lg. The object of this paper is to provide a theoretical description of the propagation of these regional phases which can be used as the basis for discussions of the effects of structure and source type. The development is based on the operator methods of Kennett (1984), to get a representation of the full wavefield in crust and mantle models with lateral variation in seismic properties. The operator results are then broken down into contributions associated with particular wavetypes using approximations introduced by Kennett (1986a). The net result is a specific description of the propagation processes contributing to Pg, Lg and Pn, Sn with inclusion of the most important interconversions between wavetypes, for a laterally heterogeneous structure.

These representations of the regional phases are then used to

-4-

examine the behaviour of some proposed discriminants between earthquakes and underground explosions based on the relative amplitudes of P and S phases. The preferred phase for use for P waves is the Pn phase because it represents a distinct arrival at the beginning of the record. The size of the later Pg phase is too dependent on the nature of the propagation path to be general useful. The ratio of the amplitudes of the Pn and Sn phases looks promising as a high frequency discriminant   for events which are large enough for Sn to be   observed clearly. However, the ratio of the amplitudes of Lg and Pn is not as useful because of the complex nature of the of the propagation characteristics of Lg in heterogeneous media.

Computations based on an implementation of the operator representation for laterally varying media via wavenumber mixing in the transform domain will be presented in a companion paper.

2. General description of regional phases

We will here show how the operator development of the seismic wavefield introduced by Kennett (1984, 1986a) can be adapted to the description of regional seismic phases.

2.1 Reflection and transmission operators

Consider a heterogeneous region bounded by smooth surfaces A ($z = f_A(x_\perp)$, $x_\perp = (x,y)$) and C ($z = f_c(x_\perp)$) which do not deviate far from horizontal planes. In order to isolate the region from its surroundings, we consider it to be bordered on each side by uniform media a, c (see fig 1). Then, if there is a downgoing wavefield D^a incident from the uniform medium a upon the region AC, the reflected field back into a is written,

$$\underset{\sim}{u}^{refl}(\underset{\sim}{x}_\perp) = R_D^{AC}(\underset{\sim}{D}^s)$$ (2.1)

where R_D^{AC} is a reflection operator for downgoing waves; and the transmitted field in c is represented as

$$\underset{\sim}{u}^{trans}(\underset{\sim}{x}_\perp) = T_D^{AC}(\underset{\sim}{D}^s).$$ (2.2)

in terms of a transmission operator T_D^{AC}. R_D^{AC}, T_D^{AC} include the effect of any multiple reflections within the region AC. For an incident upgoing wave from the uniform medium c we may similarly introduce the corresponding operators R_U^{AC}, T_U^{AC} for upgoing waves.

These reflection and transmission operators are not tied to any particular computational implementation, and include the position dependence of the reflected and transmitted wavefields. In a stratified medium the action of R_D^{AC}, T_D^{AC} can be evaluated via matrix multiplications in the frequency-wavenumber domain and subsequent inversion of the transforms. More complex reflection and transmission processes can be represented by including the action of further operators. The operator algebra is noncommutative and operators always act to their right.

Now divide the region AC by the introduction of an intermediate surface B ($z_B = f_B(\underset{\sim}{x}_\perp)$) into two subregions AB and BC. The composite reflection and transmission operators R_D^{AC}, T_D^{AC} can be represented in terms of those for the subregions as

$$R_D^{AC} = R_D^{AB} + T_U^{AB} R_D^{BC} [I - R_U^{AB} R_D^{BC}]^{-1} T_D^{AB}.$$
$$T_D^{AC} = T_D^{BC} [I - R_U^{AB} R_D^{BC}]^{-1} T_D^{AB}.$$ (2.3)

where I is the identity operator. We recall that operators act to their right and so the physical significance of each expression can be obtained by reading from right to left.

The operator inverse $[\ I - R_u^{AB}\ R_D^{BC}\ ]^{-1}$ represents all interactions between the regions AB and BC and hence all multiple reflections within AC. We will refer to $[\ I - R_u^{AB}\ R_D^{BC}\ ]^{-1}$ as the reverberation operator for the region AC.

The operator algebra has the same structural form as the reflection matrix methods for stratified media (see e.g. Kennett 1983). This correspondence arises because the reflection matrices in the transform domain are just one implementation of the operator forms. As a result, we are able to exploit a wide range of results and approximations from the stratified case with a reinterpretation of matrices as operators.

We have so far considered the reflection and transmission operators as acting on the entire incident wavefield. But within the uniform media we have supposed to border the region of interest, we can split up the wave field into three independent wave types. In isotropic media these will be P-waves, SV-waves and SH-waves, but in anisotropic media the decomposition by wavetype may not lead to readily identifiable physical character. We will however label the three wave types by P, S and H, as in Kennett (1986a) and allow for the interconversions between wavetypes arising from the nature of the medium. We can partition the operators by input and output wavetypes so that we can write e.g.

$$R_D^{AC} = \begin{pmatrix} R_{PP} & R_{PS} & R_{PH} \\ R_{SP} & R_{SS} & R_{SH} \\ R_{HP} & R_{HS} & R_{HH} \end{pmatrix}_D^{AC}, \qquad (2.4)$$

where we have adopted the convention that R_{12} represents scattering from wavetype 2 into wavetype 1 (Kennett 1983). With this convention the partitioned forms of composite operators can be constructed by equivalent rules to matrix multiplication, for

example the PP element of $R_U^{AB} \, R_D^{BC}$ is given by

$$\left(R_U^{AB} \, R_D^{BC}\right)_{PP} = R_{UPP}^{AB} \, R_{DPP}^{BC} + R_{UPS}^{AB} \, R_{DSP}^{BC} + R_{UPH}^{AB} \, R_{DHP}^{BC} . \quad (2.5)$$

Even for an isotropic medium, the action of heterogeneity will often be to produce out of plane scattering and so couple the P-SV and SH fields together.

2.2 Operator description of the seismic wavefield

In the regional phase situation we consider a source lying in the crustal zone at a level S ($z = z_S$) with the crust/mantle boundary defined by the surface C ($z_c = f_c(x_\perp)$) - fig 2. If the source was placed in a uniform medium, with the local properties at the source, it would radiate upward and downward contributions U^S, D^S . By splitting the medium at the source level, we can work in terms of reflection and transmission operators above and below the source level S and introduce the source via its upward (U^S) and downward (D^S) radiation terms. The resulting representation of the seismic wavefield takes the form

$$\underset{\sim}{u}_0 \, (\underset{\sim}{x}_\perp) = \underset{\sim}{\tilde{W}} \, T_U^{fS} \, [\, I - R_D^{SL} \, R_U^{fS} \,]^{-1} \{ \underset{\sim}{U}^S + R_D^{SL} \, \underset{\sim}{D}^S \}, \quad (2.6)$$

where SL indicates the entire region below the source level and fS indicates the zone above the source including the free surface. T_U^{fS} represents the transmission of an upgoing wave from the source level up to the free surface and $\tilde{W}$ is the surface amplification factor arising from the interference of up and downgoing wavefields at the free surface. The inverse operator $[\, I - R_D^{SL} \, R_U^{fS} \,]^{-1}$ includes all multiple interactions between the regions above and below the source. Equation (2.6) for the seismic wavefield can be rewritten in a way that emphasises the

surface reflected phases

$$\underset{\sim}{u}_b \, (\underset{\sim}{x}_1) = \quad \tilde{W} \; T_U^{fs} \, \{ \, \underset{\sim}{U}^s \, \} \qquad\qquad (2.7)$$

$$+ \; \tilde{W} \; T_U^{fs} \; [\; I - R_D^{SL} \; R_U^{fs} \;]^{-1} \; R_D^{SL} \, (\underset{\sim}{D}^S + R_U^{fs} \; \underset{\sim}{U}^S \,),$$

In this representation for the wavefield we have the reverberation operator for the entire structure combined with reflection from beneath the source level. Since we have the operator identity

$$[\; I - R_D^{SL} \; R_U^{fs} \;]^{-1} \; R_D^{SL} = \quad R_D^{SL} \; [\; I - R_U^{fs} \; R_D^{SL} \;]^{-1} \; ,$$

we can view the reverberation sequence as occurring on either the source or the receiver sides of the main reflection R_D^{SL} .

We can now begin to separate phases propagating in the crust from those with a mantle component by splitting the reflection operator R_D^{SL} just below the crust/mantle boundary C using (2.3)

$$R_D^{SL} = R_D^{SC} + T_U^{SC} \; [\; I - R_D^{CL} \; R_U^{SC} \;]^{-1} \; R_D^{CL} \; T_D^{SC} \; . \qquad (2.8)$$

This separation includes reflection of downward travelling waves at the crust-mantle interface in the crustal operator R_D^{SC} . The dominant multiples in regional propagation arise from the free surface, but there can be a contribution from a complex crust-mantle transition. We will therefore rewrite (2.8) in a form which emphasises the separation into crust and mantle operators:

$$R_D^{SL} = R_D^{SC} + T_U^{SC} \; R_D^{ML} \; T_D^{SC} \; . \qquad\qquad (2.9)$$

Here R_D^{ML} includes all mantle reflection effects, both direct reflection (R_D^{CL}) and any modulation from the effect of the structure of the crust/mantle transition through $[\; I - R_D^{CL} \; R_U^{SC} \;]^{-1}$ We would like to make use of the expansion (2.9) to separate

multiple reflections in the crustal zone from the overall reverberation operator $[\ I\ -\ R_D^{SL}\ R_U^{fs}\ ]^{-1}$. We make use of the operator identity

$$[\ I\ -\ A\ -\ B\ ]^{-1}\ =\ [\ I\ -\ A\ ]^{-1}\ +\ [\ I\ -\ A\ ]^{-1}\ B\ [\ I\ -\ A\ -\ B\ ]^{-1}.$$

which leads to an expansion in multiple powers of the operator combination $B\ [\ I\ -\ A\ ]^{-1}$. With the identification of A with $R_D^{sc}\ R_U^{fs}$ and the mantle contribution $T_U^{sc}\ R_D^{ML}\ T_D^{sc}\ R_U^{fs}$ as B, we can develop an expansion of the form

$$
\begin{aligned}
[\ I\ -\ R_D^{SL}\ R_U^{fs}\ ]^{-1}\ =\ & [\ I\ -\ R_D^{sc}\ R_U^{fs}\ ]^{-1} \\
& +\ [\ I\ -\ R_D^{sc}\ R_U^{fs}\ ]^{-1}\ T_U^{sc}\ R_D^{ML}\ T_D^{sc}\ R_U^{fs}\ [\ I\ -\ R_D^{sc}\ R_U^{fs}\ ]^{-1} \\
& +\ \ldots\ldots
\end{aligned}
\tag{2.10}
$$

and we can recognise $[\ I\ -\ R_D^{sc}\ R_U^{fs}\ ]^{-1}$ as the reverberation operator for the crust.

When we make use of the crust-mantle decomposition in (2.9) and (2.10) in the expansion for the seismic wave field (2.7) we can set up a hierachy of propagation terms emphasising the different classes of wave interaction with the structure of significance for regional phases

$$
\underline{u}_0\ (\underline{x}_L)\ =\ \ \tilde{W}\ T_U^{fs}\ \{\underline{U}^s\}
\tag{2.11a}
$$

$$
+\ \tilde{W}\ T_U^{fs}\ [\ I\ -\ R_D^{sc}\ R_U^{fs}\ ]^{-1}\ R_D^{sc}(\underline{D}^s\ +\ R_U^{fs}\ \underline{U}^s)
\tag{2.11b}
$$

$$
+\ \tilde{W}\ T_U^{fs}\ [\ I\ -\ R_D^{sc}\ R_U^{fs}\ ]^{-1}\ T_U^{sc}\ R_D^{ML}\ T_D^{sc}\ [\ I\ -\ R_U^{fs}\ R_D^{sc}\ ]^{-1}
$$
$$
\cdot(\underline{D}^s\ +\ R_U^{fs}\ \underline{U}^s)
\tag{2.11c}
$$

$$
+\ \ldots\ldots
$$

The contribution (2.11a) represents the direct waves transmitted upward from the source level. The part (2.11b) represents the crustally trapped waves such as Pg, Lg involving multiple interactions with the free surface and the crust/mantle interface.

The contribution (2.11c) represents dominantly upper mantle propagation such as Pn,Sn with the possibility of near-source or near-receiver crustal reverberations. The higher order terms involve multiple mantle interaction.

Equation (2.11) thus provides an operational description of the main regional seismic phases in terms of the propagation characteristics of the regions above and below the source. For shallow sources the natural divisions of the heterogeneity structure may well not coincide with the placing of the source. However, with a little extra effort we can generate an operator description for fixed upper and lower crustal zones; the details are presented in the Appendix. For heterogeneity superimposed on stratification the operators can be simulated by wavenumber coupling techniques in the frequency-wavenumber domain (Kennett 1986). Equation (2.11) can then be used to synthesise the response for the various phases including, for example, different scales of heterogeneity in the mantle and the parts of the crust lying above and below the source.

However, (2.11) provides a composite description of the entire seismic wavefield and provides no immediate separation into the P and S regional phases. In order to make a specific description of the individual phases Pg, Pn, Lg, Sn we need to look in detail at near source and near receiver processes and the character of the crustal reverberations.

2.1 Near-source effects

The action of the source enters the operator description of the wavefield through $(\underline{D}^s + R_u^{fs} \underline{U}^s)$ which represents the combination of the direct downward radiation from the source and reflections from above the source, which will be dominated by the effect of

the free surface.

In terms of the three basic wavetypes (P,S,H) we have the explicit expressions

$$(\underline{D}^s + R_v^{fs}\, \underline{U}^s)_P = D_P + R_{vPP}^{fs}\, U_P + R_{vPS}^{fs}\, U_S + R_{vPH}^{fs}\, U_H \, ,$$

$$(\underline{D}^s + R_v^{fs}\, \underline{U}^s)_S = D_S + R_{vSP}^{fs}\, U_P + R_{vSS}^{fs}\, U_S + R_{vSH}^{fs}\, U_H \, ,$$

$$(\underline{D}^s + R_v^{fs}\, \underline{U}^s)_H = D_H + R_{vHP}^{fs}\, U_P + R_{vHS}^{fs}\, U_S + R_{vHH}^{fs}\, U_H \, ,$$

$$(2.12)$$

allowing for full interconversion above the source.

For an explosive source, the dominant radiation will be as P in D_P , U_P and S wave contributions will be generated from free surface reflections; these would normally be mainly SV, but some SH waves could occur due to heterogeneity above the source. For a large explosion, there is also the possibility of tectonic release close to the source inducing direct S radiation. Similar effects will arise from extended or multiple sources. Thus if we consider the SV wave radiation from an explosion we can group the source contributions in terms of their likely significance:

$$C_S^{expl} = R_{USP}^{fs}\, U_P + (D_S + R_{USS}^{fs}\, U_S) + R_{USH}^{fs}\, U_H \, , \qquad (2.13)$$

the first term would be generated with a stratified medium code and a simple source model, the second term is associated with tectonic release and the third would arise almost entirely from heterogeneity effects.

For an earthquake source, we have to take account of P,SV and SH radiation at the source itself and heterogeneity will have the effect of linking the SV and SH wavefields. In this context we should note that such coupling would be predicted directly for anisotropic models. However if we adopt an isotropic reference model, the action of anisotropy and heterogeneity are formally equivalent and combined in the same operator description (although

-12-

the nature of the coupling terms will be different).

As shown in the Appendix, the effect of heterogeneity in the source zone will be to modify the effective source to $X^s (D^s + R_v^{fs} U^s)$, where X^s represents multiple scattering effects in the source region. The action of X^s will be to introduce further coupling between wavetypes. This will have the effect, for example of generating apparent downward radiation of S waves from even a simple explosion due to heterogeneity induced contributions of the type $X_{SP}^s D_P$, $X_{RP}^s D_P$.

2.2 Near-receiver effects

The receivers are normally situated at or near the free surface and so lie in a region of concentrated small-scale heterogeneity even in regions with apparently homogeneous geology. Signal generated noise from the vicinity of the receivers is frequently one of the major contaminants of high frequency seismic data. In the operational description of the seismic phases (2.11) such effects are included in the term $\tilde{W} \ T_v^{fs}$. For low frequency waves this operator will be close to that for a stratified medium. But, at high frequencies we will have to allow for significant deviations from the stratified results induced by three-dimensional velocity structure and local topography near the receivers. We will therefore need to assume that any incident wavetype at the level S can produce all three components of motion at the surface, and that wavetype coupling is likely to be significant (both in-plane e.g. P-SV and out-of-plane e.g. P-SH). Thus we will write

$$\tilde{W} \ T_v^{fs} = \begin{pmatrix} W_{ZP} & W_{ZS} & W_{ZH} \\ W_{RP} & W_{RS} & W_{RH} \\ W_{TP} & W_{TS} & W_{TH} \end{pmatrix} , \qquad (2.14)$$

in terms of displacement components on the vertical (Z), radial (R) and tangential (T) components at a receiver, for a particular wavetype incident at the level S. The character of the surface motion may well include other wavetypes than the incident. For a horizontally stratified medium W_{TP} , W_{ZH} are always zero and W_{TS} , W_{RH} would only be significant in the near-field of a source.

2.3 Reverberation expansion

As we have seen reverberation operators of the type $[I - R_{D}^{SC} R_{U}^{fS}]^{-1}$ play an important role in the description of the seismic wavefield at regional ranges. The compact representation of the operator inverse does not allow the identification of reverberation sequences associated with individual wavetypes.

The crustal reverberation operator is the inverse of $[I - R_{D}^{SC} R_{U}^{fS}]$ which can be written in partitioned form as

$$[I - R_{D}^{SC} R_{U}^{fS}] = \begin{pmatrix} X_{PP} - Y_{PP} & - Y_{PS} & - Y_{PH} \\ - Y_{SP} & X_{SS} - Y_{SS} & - Y_{SH} \\ - Y_{HP} & - Y_{HS} & X_{HH} - Y_{HH} \end{pmatrix} \quad (2.15)$$

where the diagonal terms are e.g.

$$X_{PP} = 1 - R_{DPP}^{SC} R_{UPP}^{fS} \quad , \quad Y_{PP} = R_{DPS}^{SC} R_{USP}^{fS} + R_{DPH}^{SC} R_{UHP}^{fS} , \quad (2.16)$$

and the terms involving conversions take the form

$$Y_{PS} = R_{DPP}^{SC} R_{UPS}^{fS} + R_{DPS}^{SC} R_{USS}^{fS} + R_{DPH}^{SC} R_{UHS}^{fS} . \quad (2.17)$$

Using (2.15), it is possible to construct exact expressions for the partitions of the reverberation operator in terms of the individual wavetypes (Kennett 1986, section 5.2). However,

the resulting expressions are rather complex, especially when
interaction between all three wavetypes are included.
Fortunately, multiple conversions between wavetypes are unlikely
to be of very great significance, and so we may employ a
convenient approximation to the reverberation operator in which
no more than two conversions are considered:

$$
[I - R_D^{sc} R_U^{fs}]^{-1} = \begin{pmatrix} X_{PP}^{-1} + X_{PP}^{-1} Y_{PP} X_{PP}^{-1} & X_{PP}^{-1} Y_{PS} X_{SS}^{-1} & X_{PP}^{-1} Y_{PH} X_{HH}^{-1} \\ X_{SS}^{-1} Y_{SP} X_{PP}^{-1} & X_{SS}^{-1} + X_{SS}^{-1} Y_{SS} X_{SS}^{-1} & X_{SS}^{-1} Y_{SH} X_{HH}^{-1} \\ X_{HH}^{-1} Y_{HP} X_{PP}^{-1} & X_{HH}^{-1} Y_{HS} X_{SS}^{-1} & X_{HH}^{-1} + X_{HH}^{-1} Y_{HH} X_{HH}^{-1} \end{pmatrix} .
$$

$$(2.18)$$

In this approximation we have been able to extract the
reverberation terms for the individual wavetypes X_{PP}^{-1}, X_{SS}^{-1}, X_{HH}^{-1}.
Conversions between wavetypes are accompanied by the reverberation
sequences for both primary and secondary wavetypes.

3. Representation of specific seismic phases

In the previous section we have seen how we may describe
the seismic wavefield at regional ranges with an operational
development and have also considered near-source, near-receiver
and crustal reverberation effects. With these preliminaries, we
are in a position to produce representations of specific seismic
phases. We will start with crustally guided waves and then turn
attention to those phases whose paths lie mainly in the mantle.

3.1 Crustally guided waves

The first group of waves whose paths lie in the crust is that
associated with transmission upward from the source (2.11a)

$$
\underset{\sim}{u}_e^s = \tilde{W} T_U^{fs} (\underset{\sim}{U}^s) \tag{3.1}
$$

These direct P or S waves are important close to the source, but

at greater distances are reduced in amplitude by geometrical spreading. Since the direct waves travel through the lower velocity material near the surface, they are overtaken at larger distances by phases travelling mostly through the higher velocity material at depth, and then play a fairly minor role in the coda. Of much greater significance are those waves which have been reflected back from beneath the source level and then have been involved with reverberation through the whole crustal zone (2.11b)

$$\underset{\sim}{u^c_o} = \tilde{M} \; T_v^{fs} \; [\; I - R_{\supset}^{sc} \; R_v^{fs} \;]^{-1} \; R_{\supset}^{sc} \{ \underset{\sim}{D^s} + R_v^{fs} \; \underset{\sim}{U^s} \} \; . \qquad (3.2)$$

We recall that the level C lies just below the crust-mantle transition so that $R_{\supset}^{sc}$ includes reflection from this interface (e.g. PmP, SmS arrivals). A schematic representation of the various operator interactions in (3.2) is shown in figure 3. At low frequencies, the structure beneath the interface will be involved in the reflection process and so influence the crustal reverberations (Burdick & Helmberger 1988). However, for frequencies higher than about 0.5 Hz, the representation (3.2) will include the dominant contribution to the crustally guided phases Pg,Lg. The effect of source depth will enter into the expression (3.2) through the compound source term $\{ \underset{\sim}{D^s} + R_v^{fs} \; \underset{\sim}{U^s} \}$. The balance between downward and upward waves will be of particular relevance for directional sources such as earthquakes.

With the aid of the decomposition of the crustal reverberation operator by wavetypes discussed in section 2.3, we can now look at the individual seismic phases.

3.1.1 Pg

The Pg phase is composed primarily of P waves guided in the crust although the coda is likely to have an increasing

proportion of converted waves. Conversion near the source will normally be significant in transferring S energy frc.. the source radiation to the P wavefield. The base of the weathered zone near the surface will be one of the most likely places for conversion from P to other wavetypes and so transfer energy to the tangential component. These effects can be included by making a full representation of the transmission through the surface zone (2.14). The most significant contribution to the Pg phase will be from those wave propagation processes with just P reverberations in the crust with the form

$$
\underset{\sim}{u}_{Pg} = W_P \cdot X_{PP}^{-1} \cdot [R_{DPP}^{sc} (D_P + R_{UPP}^{fs} U_P + R_{UPS}^{fs} U_S + R_{UPH}^{fs} U_H)
$$
$$
+R_{DPS}^{sc} (D_S + R_{USP}^{fs} U_P + R_{USS}^{fs} U_S)
$$
$$
+R_{DPH}^{sc} (D_H + R_{UHH}^{fs} U_H)] \tag{3.3}
$$

where X_{PP}^{-1} is the crustal reverberation operator for P waves

$$
X_{PP}^{-1} = [1 - R_{DPP}^{sc} R_{UPP}^{fs}]^{-1} . \tag{3.4}
$$

W_P is the transmission operator for the surface motion generated by an incident upward P wave at the source level

$$
W_P = [W_{ZP} , W_{RP} , W_{TP}] , \tag{3.5}
$$

this allows for scattering of energy out-of-plane and possible conversions near the surface.

The contributions to the coda of Pg involve multiple reverberation trains such as

$$
X_{PP}^{-1} Y_{PP} X_{PP}^{-1} = [1- R_{DPP}^{sc} R_{UPP}^{fs}]^{-1} (R_{DPS}^{sc} R_{VSP}^{fs} +R_{DPH}^{sc} R_{UHP}^{fs})[1- R_{DPP}^{sc} R_{UPP}^{fs}]^{-1} .
$$
$$
\tag{3.6}
$$

and similar terms with conversion between reverberations of the type

$$
X_{PP}^{-1} Y_{PS} X_{SS}^{-1} = [1- R_{DPP}^{sc} R_{UPP}^{fs}] (R_{DPP}^{sc} R_{VPS}^{fs} +R_{DPS}^{sc} R_{USS}^{fs} + R_{DPH}^{sc} R_{UHS}^{fs}) .
$$
$$
. [1- R_{DPP}^{sc} R_{UPP}^{fs}]^{-1} \tag{3.7}
$$

with those process involving SH waves likely to be of least significance. Since all these contributions require conversions between wavetypes, they are likely to be individually small but the cumulative effect of a number of such terms can still be noticeable.

The character of the Pg wavetrain will be strongly dependent on the nature of the crustal reverberation operator X_{PP}^{-1}. Multiple reflections in the crust for P provide only partial trapping of energy, because of conversion from P to S at the surface and the possibility of transmission through the crust-mantle transition into S waves in the mantle.

For laterally homogeneous crustal models, the detailed studies of Olsen et al (1983), Campillo et al (1984) have shown how the Pg phase is built up from multiple PmP reflections. However, it is difficult to sustain the Pg phase to even 500 km range if there is not low velocity material near the surface. A crustal low velocity zone may help to maintain Pg amplitudes by interference of multiples separated by only a short time delay.

In a shield type model, the Pg energy leaks rapidly into S with each surface reflection and the Pg phase tends not to be observed at large ranges. The presence of lateral heterogeneity will tend to enhance the decay of Pg with range, since scattering will generally remove energy from the waveguide. These results help to explain why Pg is more readily observed in the western United States, where surface P wave velocities tend to be low, than in the eastern United States where older geological structures bring higher velocity material close to the surface.

3.1.2 Sg, Lg

At close ranges, the crustally guided S waves, analogous to Pg, are commonly referred to as Sg. But at greater distances as the wavetrains become more complex, the notation Lg is frequently used. Originally the term Lg was applied to intermediate frequency arrivals with a group velocity around 3.5 km/s (Press & Ewing 1952), but more recently the usage has been transferred to higher frequency waves (> 1 Hz).

When considering these S wavetrains we have to take account of the different classes of wave propagation processes associated with the two S wavetypes. In a horizontally stratified, isotropic, medium the SV waves would propagate in a vertical plane and SH in a horizontal plane. The SV waves part of Lg can then be described by a superposition of many higher modes of Rayleigh waves and the SH wave part by a similar sum of Love wave terms. However, in a real medium there will be cross-coupling between the wavetypes due to out-of-plane scattering arising from heterogeneity in the crustal waveguide.

The phase velocities of importance for guided S waves are such that P waves will only propagate in the near surface region (if at all). As a result, we only need to retain P waves in the description of near-source and near-receiver processes. Within the full crustal waveguide the behaviour will be dominated by S wave reverberations, but for each wavetype we must make a full allowance for near-receiver effects including coupling to P waves and Rg waves (fundamental mode Rayleigh waves) largely confined to the near surface.

In order to simplify the notation we introduce C_{DS}, C_{DH} representing the net downward radiation for SV, SH waves including the effect of reflection processes above the source

$$C_{DS} = D_S + R_{USP}^{fs} U_P + R_{USS}^{fs} U_S + R_{USM}^{fs} U_M \quad ,$$

$$C_{DM} = D_M + R_{UMP}^{fs} U_P + R_{UMS}^{fs} U_S + R_{UMM}^{fs} U_M \quad , \tag{3.8}$$

The dominant reflection processes above the source are likely to be those without change of wavetype. The main effects of the guiding process will be described by the crustal reverberation operators for the two S wave types representing the effects of multiple internal reflections within the crust. Using the notation of section 2.3 we will write

$$X_{SS}^{-1} = [1 - R_{DSS}^{sc} R_{USS}^{fs}]^{-1} \quad ,$$

$$X_{MM}^{-1} = [1 - R_{DMM}^{sc} R_{UMM}^{fs}]^{-1} \quad . \tag{3.9}$$

Within the crustal waveguide we can expect cross-coupling between wavetypes through the terms Y_{SS}, Y_{SM}, Y_{MS}, Y_{MM} with principal contributions

$$Y_{SS} \leftarrow R_{DSM}^{sc} R_{UMS}^{fs} \quad , \qquad Y_{SM} \leftarrow R_{DSS}^{sc} R_{USM}^{fs} + R_{DSM}^{sc} R_{UMM}^{fs} \quad ,$$

$$Y_{MM} \leftarrow R_{DMS}^{sc} R_{USM}^{fs} \quad , \qquad Y_{MS} \leftarrow R_{DMS}^{sc} R_{USS}^{fs} + R_{DMM}^{sc} R_{UMS}^{fs} \quad , \tag{3.10}$$

and terms of lower importance involving P wave conversion. We must allow for full coupling in propagation through the near-surface zone. For incident S waves the two transmission terms can be represented as

$$W_S = [W_{ZS} , W_{RS} , W_{TS}] \quad ,$$

$$W_M = [W_{ZM} , W_{RM} , W_{TM}] \quad , \tag{3.11}$$

with allowance for transfer of energy out-of-plane.

The Lg wavetrains can then be split into two classes depending on the nature of the main sequence of multiple S wave reflections. Within the waveguide, cross-coupling between wavetypes will increase the complexity of the wavepropagation process. With dominantly SV reverberation, the major contributions to Lg can be

written as

$$\underset{\sim}{u}_{LgS} = W_S \cdot X_{SS}^{-1} \; [\; (R_{DSS}^{sc} + Y_{SS} X_{SS}^{-1} R_{DSS}^{sc} + Y_{SH} X_{HH}^{-1} R_{DHS}^{sc}) \; C_{DS}$$
$$+ (R_{DSH}^{sc} + Y_{SS} X_{SS}^{-1} R_{DSH}^{sc} + Y_{SH} X_{HH}^{-1} R_{DHH}^{sc}) \; C_{DH}],$$

(3.12a)

with a similar form for the dominantly SH wave propagation

$$\underset{\sim}{u}_{LgH} = W_H \cdot X_{HH}^{-1} \; [\; (R_{DHS}^{sc} + Y_{HS} X_{SS}^{-1} R_{DSS}^{sc} + Y_{HH} X_{HH}^{-1} R_{DHS}^{sc}) \; C_{DS}$$
$$+ (R_{DHH}^{sc} + Y_{HS} X_{SS}^{-1} R_{DSH}^{sc} + Y_{HH} X_{HH}^{-1} R_{DHH}^{sc}) \; C_{DH}],$$

(3.12b)

Because the wavespeeds of the different wavetypes are so similar, we need to retain a more complete representation than for Pg. However, the main effects will arise from terms with a single reverberation sequence.

For the Lg phases, the trapping of S energy is quite efficient. In the laterally homogeneous case, there will be total reflection of S waves at the surface and at a crust-mantle interface; some slight energy loss may arise at the base of the crust for a transitional structure into the mantle. Even in the presence of lateral heterogeneity most of the energy will be trapped. There will be some energy loss by anelastic attenuation and scattering and so the reverberation sequences X_{SS}^{-1}, X_{HH}^{-1} will decay in time. This leads to a general reduction of the coda amplitude along the wavetrain as time progresses, whose envelope can usually be approximated by an exponential to define a coda Q (Herrmann 1980).

There are a number of regions where the propagation of the Lg wave is interrupted by some tectonic feature e.g. the graben structure in the North Sea (Gregersen 1984) and the mountain belts of central Asia (Ruzaikin et al, 1977). This disruption of the wavetrain is generally associated with upsetting the constructive

interference of the multiple crustal S reflections comprising X_{SS}^{-1} , X_{MM}^{-1} . As illustrated by Kennett (1986b), modifications of the shape of the crustal waveguide tend to break up the constructive interference and these trends will be enhanced by significant horizontal velocity gradients. In addition anomalously low Q may be needed to finally extinguish the guided energy (Maupin 1989).

3.2 Mantle phases

Once we get beyond the critical distance for reflection from the crust-mantle transition, we have the possibility of phases with a significant path in the mantle associated with operator (2.9) , which includes all reflection from beneath our separation level C (just below the crust-mantle inter ce). The general description of such mantle phases is provided by (2.11c)

$$\underset{\sim M}{u} = \tilde{W} \; T_v^{fs} \; [\; I - R_{\mathfrak{d}}^{sc} \; R_v^{fs} \;]^{-1} \; T_v^{sc} \; R_{\mathfrak{d}}^{ml} \; T_{\mathfrak{d}}^{sc} \; [\; I - R_v^{fs} \; R_{\mathfrak{d}}^{sc} \;]^{-1}$$
$$\cdot (\underset{\sim}{D}^s + R_v^{fs} \; \underset{\sim}{U}^s) \; , \tag{3.13}$$

which includes the possibility of reverberations in the crust near the source or near the receiver. We recall that $R_{\mathfrak{d}}^{ml}$ is a contracted notation

$$R_{\mathfrak{d}}^{ml} = R_{\mathfrak{d}}^{cl} \; [\; I - R_{\mathfrak{d}}^{cl} \; R_v^{sc} \;]^{-1} \; ,$$

designed to include all mantle reflections including those arising from the structure of the crust-mantle transition zone. As in (3.2) the effect of source depth enters into the expression for the wavefield through the compound source term $(\underset{-}{D}^s + R_v^{fs} \underset{-}{U}^s)$.

We can extract the main term corresponding to Pn, Sn from (3.13) as

$$\underset{\sim R}{u} = \tilde{W} \; T_v^{fs} \cdot T_v^{sc} \; R_{\mathfrak{d}}^{ml} \; T_{\mathfrak{d}}^{sc} \cdot (\underset{\sim}{D}^s + R_v^{fs} \; \underset{\sim}{U}^s) \tag{3.14}$$

which includes the possibility of reflections from the surface at the source e.g. pPn, sSn (see fig 4). The coda of these two phases will include crustal multiples such as PPn, SSn.

3.2.1 Pn

The beginning of the Pn wavetrain will be dominated by P waves radiated downward from the source, with some reinforcement slightly later from surface reflected phases (including S to P conversion) for shallow sources. The mantle leg will be as a P wave so that we may represent the wavetrain as

$$
\underset{\sim}{u}_{Pn} = W_P \, T_{UPP}^{sc} \, R_{DPP}^{ML} \, T_{DPP}^{sc} \, \{ D_P + R_{UPP}^{fs} \, U_P + R_{UPS}^{fs} \, U_s + R_{UPM}^{fs} \, U_M \},
$$

$$(3.15)$$

where cross-coupling between wavetypes in the near-surface zone is included via the transmission term W_P (3.5).

At ranges beyond 300-400 km, crustal multiples of Pn begin to contribute to the coda of Pn as indicated in the representation (3.13). For the range of phase velocites of importance for this phase 8.3-7.8 km/s, conversion of P to S waves at the surface is more efficient than reflection of P to itself so that some crustal legs may be as S waves. As a result the Pn coda will begin to acquire a partial S wave character.

3.2.2 Sn

The principal phase velocity interval for Sn (4.8-4.3 km/s) will involve only limited interaction with P waves in the near surface zone and so we only need to consider S wave propagation over the bulk of the path. The most significant other class of wavetype conversion is likely to be between the two S waves, induced by the presence of heterogeneity. We will therefore compound the transmission up and down below the source level with the mantle reflection processes into a composite operator

$$R_{\mathcal{D}}^{SM} = T_U^{sc} \, R_{\mathcal{D}}^{ML} \, T_{\mathcal{D}}^{sc} \, , \tag{3.16}$$

and then partition the whole process by incident and emergent wavetype. Then, with the aid of the compact effective source notation introduced in section 3.1.2 we can represent the dominantly SV wave contribution to Sn as

$$\underset{\sim}{u}_{S_nS} = W_S \cdot (\, R_{\mathcal{D}SS}^{SM} \, C_{\mathcal{D}S} + R_{\mathcal{D}SH}^{SM} \, C_{\mathcal{D}H} \,) \, , \tag{3.17}$$

with an equivalent form for the SH wave contribution

$$\underset{\sim}{u}_{S_nH} = W_H \cdot (\, R_{\mathcal{D}HS}^{SM} \, C_{\mathcal{D}S} + R_{\mathcal{D}HH}^{SM} \, C_{\mathcal{D}H} \,) \, , \tag{3.18}$$

As for Pn, the coda of Sn will include crustal multiples. Since reflection at the surface involves only limited coupling to P, this will be a relatively efficient process and as such a major contributor to the character of Sn at larger ranges (Kennett 1985).

Although the various operator descriptions take similar forms for the crustally guided and mantle waves, we must recall that the ranges of phase velocity for which the representations are useful are rather different. We have been able to partition the seismic wavefield via the dominant modes of propagation, but we must recall that the phases do not exist in isolation. Thus the Sn and Lg arrivals are superimposed on the Pg coda and the spectral character of the actual wavefield can be dominated by coda contamination (Blandford 1980). Also, we have included all mantle propagation effects within the Pn,Sn representations, energy return from structure well below the crust/mantle interface can be of considerable importance at larger ranges and may well occur in a time window that, for an isolated record, could be confused with the crustal multiples of shallower propagating energy.

4. P/S amplitude ratios for regional phases

With these relatively compact descriptions of the regional
seismic phases, we are now in a position to look at the behaviour
of possible discriminants between different types of seismic
sources. For discrimination between earthquakes and explosions,
such criteria are based on the observation that earthquakes should
be much more efficient generators of S waves than explosions, as
demonstrated very elegantly by Gilbert (1973). For regional
phases this result implies that we would, in general, expect
larger amplitude Sn and Lg phases relative to the size of the P
waves for earthquakes than explosions. Some earthquake
observations near nodes in the source radiation patterns could be
deceptive, but with a reasonable coverage of azimuths such
problems should be avoided.

Such discrimination criteria based on the relative amplitudes
of P and S regional phases have been investigated for some time
but their performance has been somewhat mixed. Blandford (1980)
argues strongly for the the use of the ratio of the maximum
amplitude before Sn (Pmax) to the maximum after Sn (Lg),
particularly at high frequencies. However, Pomeroy et al (1982)
report on a range of other observations which are not as
encouraging. Clearly, it is desirable to look at the theoretical
basis for the discriminant to see if we can understand where the
problems arise.

4.1 Sn/Pn amplitude ratio

This amplitude ratio is designed to compare the Pn and Sn
phases which both have a significant mantle component to the
propagation path. Pn has the advantage that it appears as a first

arrival and only contends with the ambient noise conditions. Sn, on the other hand, is superimposed on the late P coda and frequently has a relatively emergent character with the largest energy on the vertical component often associated with crustal multiples (Kennett 1985). Over continental areas Sn usually propagates well, although there is some disruption due to tectonic features (Molnar & Oliver 1969).

In the absence of widespread digital three-component stations the amplitude comparison of Pn and Sn is normally made on the vertical component. Thus from equations (3.15), the vertical component of Pn will be represented by

$$w_{Pn} = W_{ZP} R_{DPP}^{sm} (D_P + R_{UPP}^{fs} U_P + R_{UPS}^{fs} U_S), \tag{4.1}$$

with a phase velocity window of interest from 7.8-8.3 km/s. For shallow sources there will be the complication that the time separation of direct downward radiation and surface reflections will be too short to allow separate identification except at high frequency.

From (3.17,3.18) the vertical component of the Sn phase will be described by

$$w_{Sn} = (W_{ZS} R_{DSS}^{sm} + W_{ZH} R_{DHS}^{sm})(D_S + R_{USP}^{fs} U_P + R_{USS}^{fs} U_S)$$
$$+(W_{ZS} R_{DSH}^{sm} + W_{SH} R_{DHH}^{sm})(D_H + R_{UHP}^{fs} U_P + R_{UHH}^{fs} U_H), \tag{4.2}$$

for phase velocities from 4.1-4.7 km/s. If the level of heterogeneity is not too high the dominant propagation should remain 'in plane', with a consequent simplification of the expression for the vertical component of Sn:

$$w_{Sn} = W_{ZS} R_{DSS}^{sm} (D_S + R_{USS}^{fs} U_S + R_{USP}^{fs} U_P), \tag{4.3}$$

The out-of-plane scattering terms are particularly important for

explosions, as recognised by Gupta & Blandford (1983), since in this case the SH energy produced at the source will be low. Even with equal efficiency of scattering back and forth between SV and SH, there will be transfer of energy into the SH field until the size of the SV and SH terms tend to equalise. For earthquake sources similar cross-conversions of wavetype will occur but will be harder to recognise because of the presence of significant SH energy generated at the source.

Within the mantle the character of the propagation terms R_{DPP}^{SH}, R_{DSS}^{SH} is dictated by the wavespeed gradients beneath the Moho. Even a slight positive gradient is sufficient to produce an 'interference' head wave in which multiple reflections from the gradient constructively interfere to give a larger arrival than is possible with just a uniform zone (Menke & Richards 1980). As the range increases the deepest penetrating 'diving' ray separates from the bunch of multiple reflections near the crust-mantle interface and may get suppressed by interaction with a wavespeed inversion at depth. With fine scale structure in the mantle, the interaction of the P and S waves will be different because of the shorter wavelengths for S.

Comparing (4.1) and (4.3), we see that they have a similar structure of propagation terms. Loss of energy by out-of-plane scattering will tend to reduce the Sn mantle componment somewhat and also the transfer to the vertical component is less efficient than for P waves. The ratio of the Pn and Sn amplitudes should however be dominated by the ratio of the source terms in (4.1) and (4.3).

At high frequencies, the P wave contribution to (4.3) will be very small for the phase velocities in Sn (unless the source is very shallow), so that the Sn/Pn ratio becomes a

comparison of S and P radiation at similar take off angles from the source. At lower frequencies, and for shallow sources, the interference of PS conversion at the surface with the direct downward S radiation would complicate the picture. For explosions, this conversion process will be the principal mechanism for the generation of Sn.

This would suggest that the Pn/Sn ratio would perform better as a discriminant between earthquakes and explosions at higher frequencies, which would fit in with a number of observations (R. Blandford – private communication). For shallow earthquakes the discriminant would not be very effective. Clearly, adequate azimuthal coverage is needed to eliminate complications due to source radiation patterns.

The actual behaviour of the ratio will be affected by the presence of heterogeneity. Contamination of the arrivals by near-receiver scattering can be overcome by integrating the envelope of the waveforms over a time window rather than just picking a maximum value. Where available, three component data should be used to try to stabilise the measure of the ratio of energy in Sn and Pn against distortion due to energy transfer between the vertical and horizontal planes due to scattering.

Further, in order to equalise the sensitivity of the Pn,Sn phases to structure (particularly the effects of heterogeneity) it would be appropriate to work at a common wavelength e.g. make a comparison between Pn in a frequency band around 4 Hz with Sn in a frequency band around 2.5 Hz.

4.2 Lg/Pn amplitude ratio

Although it would be most appropriate to compare the amplitudes of the two crustally guided waves Pg, Lg, we have noted above that

the Pg phase does not propagate very far in structures with high P
wave velocity at the surface (such as shields). For utility in a
wide range of geologic environments, it is therefore necessary to
use the Pn phase as a measure of the strength of the P wave field,
except at short ranges.

With a comparable approximation to (4.3) the vertical component
of Lg associated with in-plane propagation can be derived from
(3.12) as

$$W_{Lg} = W_{zs} \, X_{ss}^{-1} \, R_{2ss}^{sc} \, \{ \, D_s + R_{uss}^{fs} \, U_s + R_{usp}^{fs} \, U_p \, \} \, , \qquad (4.4)$$

for the phase velocity range 3.8-3.3 km/s. The propagation term
now involves reflection from the crust/mantle interface in R
and reverberations within the waveguide X_{ss}^{-1} . The coherence of
the Lg phase depends on a complex pattern of constructive
interference which is normally well established at frequencies
around 1Hz, except where some major barrier blocks propagation.
Deep reflection soundings of the crust often show very variable
structure at the crust/mantle transition along a profile and so at
high frequency (> 5 Hz) the propagation effects will tend to get more
complex.

Comparison of the source terms in (4.1) and (4.4) shows a
similar behaviour to that for Sn/Pn with a simplification at
higher frequencies, although now the Pn waves will have much steeper
take-off angles than for the S waves. The waves comprising Lg
travel at angles of about 70 degrees to the vertical, whereas the
Pn takeoff angle would be between 25 and 45 degrees depending on
the depth of the source.

The Lg/Pn amplitude ratios will therefore be subject to two
opposing trends, the source ratios will be becoming better defined
as frequency increases but the propagation complexity will

increase markedly making the interpretation of the ratio rather difficult. This result supports the discordant observations of the value of the amplitude ratio Lg/Pn as a discriminant noted by Pomeroy et al (1982).

The Lg wave has a valuable role to play in the detection of events at regional ranges, but the relatively complicated propagation characteristics for Lg reduce its value for discrimination.

5. Discussion

In this paper we have shown how an economical and informative representation of the seismic wavefield at regional distances can be made in terms of reflection and transmission operators. The expressions we have derived for the various regional phases are valid in laterally heterogeneous and anisotropic media. For the particular case of a horizontally stratified media they can be readily evaluated by adapting matrix methods in the transform domain (see e.g. Kennett (1983)). In the presence of heterogeneity the operators can be simulated by allowing coupling between horizontal wavenumbers in the frequency domain. Preliminary calculations show that it is possible to achieve significant transverse components for the regional S wavefield from an explosive source as has been frequently observed (Blandford 1980), but which is not predicted by a stratified model.

We have demonstrated how operator representations for particular seismic phases can be applied to look at the theoretical basis for discrimination between earthquakes and underground nuclear explosions using regional phases. A number of empirical discriminants have been proposed based on the characteristics of regional phases (see Pomeroy et al (1982)).

Our phase representations give a way of examining the theoretical basis of such discriminants amd may allow a better assessment of their limitations.

Appendix: Upper and lower crustal heterogeneity zones

In section 2 we have shown how the propagation characteristics for regional phases can be described in terms of the regions above and below the source. Frequently, we would like to work with fixed regions irrespective of source depth, so that we can model an upper crustal zone of heterogeneity down to a level z_K, underlain by a lower crustal zone and the mantle. We will assume that the source level z_S lies above z_K and will show how we may make a representation of the wavefield equivalent to (2.11) with a separation of the propagation characteristics at the level K.

If we had a source at the level K, the displacement field could be written in an analogous form to (2.7)

$$
\underset{\sim}{u}_o \, (\underset{\sim}{x}_{\perp}) = \quad \tilde{W} \quad T_U^{fK} \, \{ \underset{\sim}{U}^K \} \tag{A.1}
$$
$$
+ \, \tilde{W} \quad T_U^{fK} \, [\, I - R_D^{KL} \, R_U^{fK} \,]^{-1} \, R_D^{KL} \, (\underset{\sim}{D}^K + R_U^{fK} \, \underset{\sim}{U}^K),
$$

and we could then make a separation of the crustal propagation terms as in equations (2.8-2.10) in terms of the artificial source level K.

In order to incorporate the effects of the true source at S we have to relate the apparent source terms $\underset{\sim}{U}^K$ and $\underset{\sim}{D}^K + R_U^{fK} \, \underset{\sim}{U}^K$ to the actual source radiation. Fortunately, we can exploit the formal equivalence with reflection matrix results for splitting the response of stratified media (Kennett 1983, section 9.2). We find for the net downgoing field

$$\underset{\sim}{C}_{D}^{K} = \underset{\sim}{D}^{K} + R_{U}^{fK} \, \underset{\sim}{U}^{K}$$
$$= T_{D}^{SK} \, [\, I - R_{U}^{fS} \, R_{D}^{SK} \,]^{-1} \, \{ \underset{\sim}{D}^{S} + R_{U}^{fS} \, \underset{\sim}{U}^{S} \} \, , \qquad (A.2)$$

For the upgoing wavefield at K, it is best to look at the full propagation term

$$\widetilde{W} \, T_{U}^{fK} \{ \underset{\sim}{U}^{K} \} = \widetilde{W} \, T_{U}^{fS} \, [\, I - R_{D}^{SK} \, R_{U}^{fS} \,]^{-1} \, \{ \underset{\sim}{U}^{S} + R_{D}^{SK} \, \underset{\sim}{D}^{S} \}, \quad (A.3)$$

which we may recast into a form where we can extract the direct upgoing wave:

$$\widetilde{W} \, T_{U}^{fK} \{ \underset{\sim}{U}^{K} \} = \widetilde{W} \, T_{U}^{fS} \{ \underset{\sim}{U}^{S} \}$$
$$+ \widetilde{W} \, T_{U}^{fS} \, R_{D}^{SK} [\, I - R_{U}^{fS} \, R_{D}^{SK} \,]^{-1} \, \{ \underset{\sim}{D}^{S} + R_{U}^{fS} \, \underset{\sim}{U}^{S} \},$$
$$(A.4)$$

In general we would not expect R_{D}^{SK} to be too large so that the direct wave would be the dominant contribution. In both (A.2) and (A.4) we can recognise a modified source term

$$[\, I - R_{U}^{fS} \, R_{D}^{SK} \,]^{-1} \, \{ \underset{\sim}{D}^{S} + R_{U}^{fS} \, \underset{\sim}{U}^{S} \}$$

representing the effect of multiple interactions with heterogeneity in the vicinity of the source.

On the receiver side, we can also expand out the upward propagation term $\widetilde{W} \, T_{U}^{fK}$ to indicate the multiple interactions with the shallow heterogeneity

$$\widetilde{W} \, T_{U}^{fK} = \widetilde{W} \, T_{U}^{fS} \, [\, I - R_{D}^{SK} \, R_{U}^{fS} \,]^{-1} \, T_{U}^{SK} \, . \qquad (A.5)$$

The reverberation term will be responsible for most of the conversions between wavetypes near the receiver.

With these expressions for the effect of shallow heterogeneity, we can rewrite the operational description of crustally guided waves (such as Pg, Lg) into the form

$$\underset{\sim}{u}^{crust} = \widetilde{W} \, T_{U}^{fK} \, . \, [\, I - R_{D}^{KC} \, R_{U}^{fK} \,]^{-1} \, R_{D}^{KC} \, . \, \underset{\sim}{C}_{D}^{K} \, , \qquad (A.6)$$

-32-

with the main propagation characteristics determined by the
multiple reverberations within the crust described by
$[I - R_D^{\kappa c} R_u^{f\kappa}]^{-1}$. For those phases with a dominant mantle path
(Pn, Sn) we have a comparable form

$$\underset{\sim}{u}^{mant} = \underset{\sim}{\widetilde{W}} \; T_u^{f\kappa} \; . \; [I - R_D^{\kappa c} R_u^{f\kappa}]^{-1} \; T_u^{\kappa c} \; R_D^{\kappa c} \; T_D^{\kappa c} \; . \; \underset{\sim}{C}_D^{\kappa} , \quad (A.7)$$

with the mantle propagation operator $R_D^{\kappa L}$ modulated by possible
crustal reverberations, and the possibility of strong interactions
with heterogeneity in the near-source ($\underset{\sim}{C}_D^{\kappa}$) and near-receiver
($\underset{\sim}{\widetilde{W}} \; T_u^{f\kappa}$) contributions.

Acknowledgement

References

Blandford R.R. (1980) Seismic discrimination problems at regional
    distances, in *Identification of Seismic Sources - Earthquake
    or Underground Explosion*, (ed. E.S. Husebye & S. Mykkeltveit),
    695-740, D. Reidel, Dordrecht

Burdick L.J. & Helmberger D.V. (1988) The discrimination potential
    of crustal resonance phases.
    AFGL Technical Report, 88-0054 (ADA196096)

Campillo M., Bouchon M. & Massinon B. (1984) Theoretical study of
    the excitation, spectral characteristics and geometrical
    attenuation of regional seismic phases,

Bull seism Soc Am 74, 79-90

Fuchs K. & Müller G. (1971) Computation of synthetic seismograms
with the reflectivity method and comparison with observations,
Geophys J R astr Soc 23, 417-433

Gilbert F. (1973) The relative efficiency of earthquakes and
explosions in exciting surface waves and body waves,
Geophys.J R astr Soc, 33, 487-488

Gregersen S. (1984) Lg wave propagation and crustal structure
differences near Denmark and the North Sea,
Geophys J R astr Soc 79, 217-234

Gupta I.N. & Blandford R.R. (1983) A mechanism for the generation
of short-period transverse motion from explosions,
Bull seism Soc Am 73, 571-591

Herrmann R.B. (1980) Q estimates using the coda of local
earthquakes, *Bull seism Soc Am*, 70, 447-468

Kennett B.L.N. (1983) *Seismic Wave Propagation in Stratified
Media*, Cambridge University Press, Cambridge

Kennett B.L.N. (1984) Reflection operator methods for elastic waves
II - composite regions and source problems,
Wave Motion 6, 419-429

Kennett B.L.N. (1985) On regional S,
Bull seism Soc Am 75, 1077-1085

Kennett B.L.N. (1986a) Wavenumber and wavetype coupling in
laterally heterogeneous media,
Geophys J R astr Soc 87, 313-331

Kennett B.L.N. (1986b) Lg waves and structural boundaries,
Bull seism Soc Am 76, 1133-1141

Maupin V. (1989) Numerical modelling of Lg wave propagation across
the North Sea Central Graben,
Geophys J R astr Soc, in press

Menke W.H. & Richards P.G. (1980) Crust-mantle whispering gallery
    phases: A deterministic model of teleseismic Pn wave
    propagation, *J geophys Res* **85**, 5416-5422

Mohorovičić A. (1909) Das Beben von 8. Okt. 1909,
    Jahrb meterol Obs Zagreb (Agram) **9**, Teil IV

Molnar P. & Oliver J. (1969) Lateral variations of attenuation in
    the upper mantle and discontinuities in the lithosphere,
    J geophys Res **74**, 2648-2682

Olsen K.H., Braile L. & Stewart J.N. (1983) Modeling short-period
    crustal phases ($\bar{P}$, Lg) for long range refraction profiles,
    Phys Earth Plan Int **31**, 334-347

Pomeroy P.W., Best W.J. & McEvilly T.J. (1982) Test ban treaty
    verification with regional data - a review
    Bull seism Soc Am **72**, S89-S129

Press F. & Ewing M. (1952) Two slow surface waves across North
    America, *Bull seism Soc Am*, **42**, 219-228

Ruzaikin A.I., Nersesov I.L., Khalturin V.I. & Molnar P. (1977)
    Propagation of Lg and lateral variations in crustal structure
    in Asia, *J geophys Res* **82**, 307-316

Figure Captions

1. Configuration of regions and surfaces for the definition of
   reflection and transmission operators.
2. Schematic representation of the action of reflection and
   transmission operators in the representation of the seismic
   wavefield.
3. Schematic representation of the operator representation for
   crustally guided waves (3.2).
4. Schematic representation of the operator representation for
   the main mantle phases (3.14).
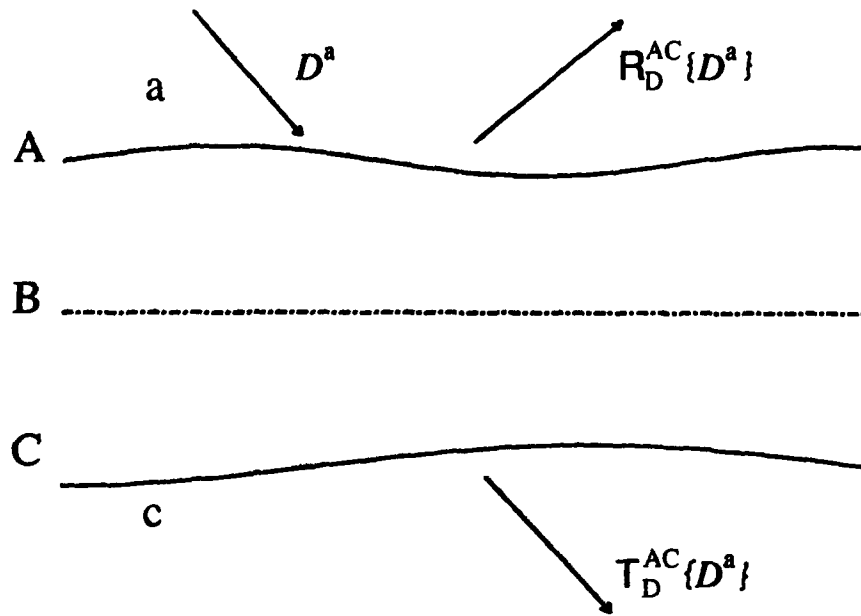
FIGURE 1
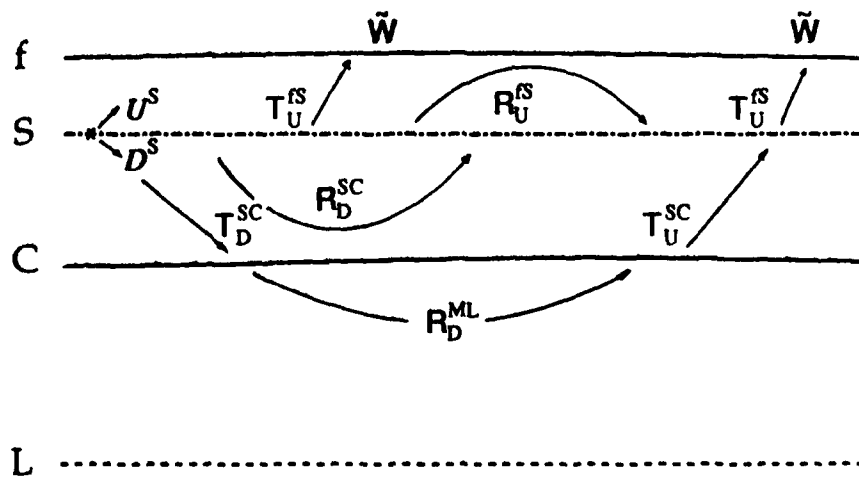
FIGURE 2
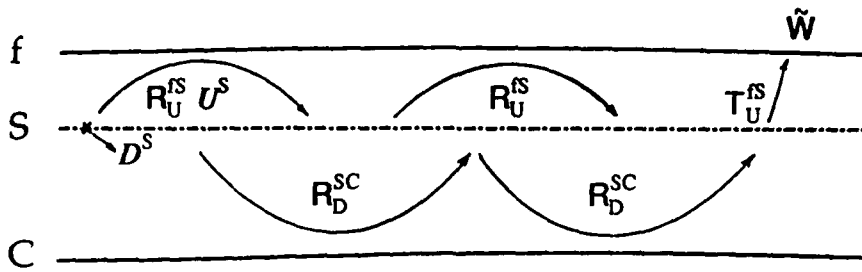
FIGURE 3
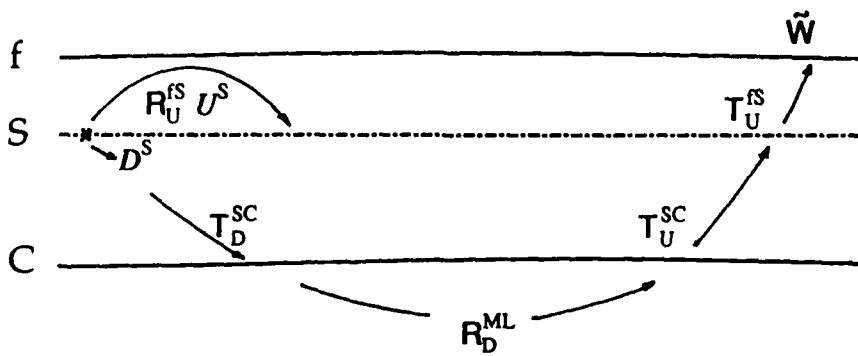
FIGURE 4

Lg-Wave Propagation in Heterogeneous Media

B.L.N. Kennett
Research School of Earth Sciences,
Australian National University
G.P.O. Box 4, Canberra, A.C.T. 2601,
Australia

ABSTRACT

The Lg wave phase which is of considerable interest for nuclear discrimination problems is normally observed after propagation through a few hundred kilometres. This phase is dominantly guided in the crustal waveguide, which is known to be a region with very significant horizontal variability in properties.

The effect of heterogeneous crustal structures on Lg waves has been determined by using a "coupled-mode" technique in which the local seismic wavefield in the real medium is expressed as a horizontally varying combination of the modal eigenfunctions of a stratified reference structure. Departures of the seismic properties in the medium from those of the reference medium lead to coupling between the various amplitude coefficients in the modal expansion. The evolution of these modal weighting factors with horizontal position are described by a coupled set of ordinary differential equations. This approach provides a calculation scheme for studying guided wave propagation over extended distances, at frequencies of 1 Hz and above. The heterogeneity models which have been used are two-dimensional and calculations are carried out for one frequency at a time.

A sequence of models with varying levels of heterogeneity have been considered in order to determine the merits and limitations of the computation scheme. The coupled mode technique works well with heterogeneous models in which the local seismic velocities differ from the stratified reference model by up to 2 per cent and there are no significant distortions of the main discontinuities (e.g. the crust-mantle boundary). The approach can be used for higher levels of heterogeneity and with distorted interfaces but a large number of modes needs to be considered with consequent high computation costs. If the level of heterogeneity is not too large then the interaction between modes can be restricted, rather than extending over the whole mode set, with consequent reduction in computation cost.

One of the major effects of crustal heterogeneity is to introduce the possibility of smearing out the main amplitude peak in the Lg wave train over a band of group velocities. As a result, an effective measure of the energy content of the Lg waves will be to consider the integrated amplitude along the trace beween group velocities of 3.6 and 3.3 km/s. The effects of heterogeneity vary between different parts of the Lg wave train and the representation of the wavefield in terms of modal contributions allows a detailed analysis in terms of the group velocity components, which can be illustrated by constructing theoretical seismograms (with a narrow bandwidth in frequency) for the heterogeneous models.

INTRODUCTION

Regional S phases have been the focus of considerable attention in recent years in the context of nuclear discrimination problems (see e.g Pomeroy, Best & McEvilly (1982)). The Sn and Lg wave trains are well established by about 200 km from the source and can frequently be followed out to ranges of 1000 km or more. These S phases travel through the crust and uppermost mantle which from a variety of studies, are known to be regions with very considerable horizontal variability in properties. In order to improve understanding of the nature of regional seismic phases and the way in which the characteristics imposed by the source may be modified by propagation to the receiever, we need a computational procedure which will allow the tracking of guided seismic wave propagation through a horizontally heterogeneous crust for a thousand kilometres. A suitable candidate is the coupled mode scheme described by Kennett (1984) which has already been used with some success in understanding the characteristics of Lg wave behaviour (Kennett & Mykkeltveit 1984).

For regional S wave trains, a representation in terms of a limited number of discrete modes gives a economical computational description for horizontally stratified media. At each frequency only a limited number of such modes need be considered. In a laterally heterogeneous medium, at a single frequency, it is possible to represent the seismic displacement and traction fields within the varying medium as a sum of contributions from the modal eigenfunctions of a reference structure, with coefficients which vary with position. The evolution of these modal expansion coefficient terms with horizontal position can be described by a set of coupled partial differential equations in the horizontal coordinates (Kennett 1984). The cross-coupling terms between different modes depend on the departures of the heterogeneous structure from the stratified reference model. These differences are not required to be very small but must not be such as to completely change the nature of the crustal wave guide. Thus, it is possible to accommodate substantial localised change in seismic velocities and density, but more difficult to allow for shifts of more than 2-3 km in the position of major interfaces such as the crust-mantle boundary. Maupin & Kennett (1987) give an extended discussion of the circumstances in which the coupled mode approach can be applied to two-dimensional heterogeneous models.

STUDIES OF TWO-DIMENSIONAL HETEROGENEITY IN THE CRUST AND MANTLE

When the heterogeneity within the medium is two-dimensional, the calculations can be recast as the solution of non-linear differential equations of Ricatti type for the reflection and transmission matrices connecting the modal expansion coefficients at different positions (Kennett 1984). The advantage of this rearrangement is that, for each frequency, the boundary conditions on the differential equations are simplified for a generally heterogeneous medium.

If we adopt a reference medium which does not vary with horizontal position, the individual mode contributions propagate independently in that structure. However, once the properties of the true medium differ from the reference, the independence of modal propagation is lost. The effect of the heterogeneity enters into the differential equations for the modal expansion coefficients via a coupling matrix whose dimensions are dictated by the number of modes included in the calculation. The choice of the number of modes is of considerable importance. All the significant wavenumber components for the seismic phase of interest should be included, as well as an allowance for steeper angles of propagation than would be present in the reference medium, in order to allow for scattering effects. The demands of computation are that the number of modes should be kept as small as possible, since the computation time depends on the square of the number of modes. On the other hand if the truncation is too tight, a poor representation of the displacement field can ensue and the results are of limited use.

In figure 1 we illustrate the reference model (ARANDA) used for most of the Lg mode calculations, and the modal eigenfunctions for the 22 Love and Rayleigh modes included in

calculations at 1.5 Hz. The vertical component of the Rayleigh modes are displayed to illustrate their very similar depth dependence to the horizontal component of the Love modes. The cut-off criterion was based on the effective depth penetration of the modes. The fundamental and first higher modes are confined to the sedimentary zone. Modes 2 to 15 are the main contributors to the Lg phase with nearly all their energy trapped in the crust. Mode 16 begins to have significant displacement in the mantle, and the remaining modes carry their main energy in the mantle and represent the Sn phase. The truncation is made at a phase velocity of 4.54 km/s, corresponding in this model to a penetration depth of about 100 km. Features in the wave propagation process corresponding to higher phase velocities than 4.54 km/s cannot be represented by these coupled mode calculations.

In order to give a good account of the guided wave propagation, we must make sure that all the significant wavenumber components for the seismic phases of interest are included, as well as making an additional allowance for steeper angles of propagation in order to allow for scattering effects. This means that we cannot just use those modes which have the bulk of their energy within the crust but must also include waves with higher phase velocity whose energy in the stratified reference model lies dominantly in the upper mantle. At 1.5 Hz, we need to carry at least the 22 modes illustrated if we are to allow for wave interaction processes generating waves travelling at angles up to 40° from the horizontal in the midcrust and even then we will not give a full account of waves travelling at steeper angles to the horizontal.

Significant perturbations of the major interfaces in the model lead to extensive coupling between modes and can induce relatively steep angles of propagation (Maupin & Kennett 1987). If such features are required in the models to be considered, then a broad sweep of modes must be taken for the reference model (for the Lg case at 1.5 Hz, at least 30). With the benefit of hindsight, it would appear that the structural model used in the calculations of Kennett & Mykkeltveit (1984) on the influence of graben structures on Lg, was as large a deviation from the reference model as could be treated effectively using their 20 mode set.

The coupled mode representation is well suited to heterogeneous models where the behaviour consists of relatively random variations about the properties of the reference model (see e.g. fig 2). In this case, a single incident mode will interact with a limited number of neighbouring modes so that the coupling matrix is dominated by the diagonal elements, with a limited effective bandwidth. With the aid of the coupled mode technique, a study has been made of the way in which the modal field for Lg waves is affected by various levels of distributed heterogeneity for frequencies up to 2Hz over paths of 100 to 1000 km long with both long and short horizontal scales of heterogeneity within the crust and mantle.

Broad Scale Heterogeneity

We will firstly describe simulations of long range propagation, for which a sequence of different heterogeneity models were constructed by specifying the seismic velocities at 40 km horizontal intervals, for a sequence of depths in a vertical section and then using bicubic spline interpolation within each layer. For the distributed heterogeneity models the velocity values were generated with a random perturbation to the reference value within a prescribed range of variation. The velocity values were then smoothed horizontally by applying a moving average over 3 points to avoid extreme variations with short horizontal scales. The horizontal smoothing process imposes a typical horizontal scale length of around 100 km, and the vertical scale varies within the model becoming larger in the upper mantle. The velocity distribution is arranged so that there are no deviations from the reference structure at the ends of the model (0 and 1000 km). This enables a direct physical interpretation of the mode coupling results, after passage through the heterogeneous region, in terms of the reflection and transmission of the modes of the reference structure.

In figure 2 we illustrate a set of models (D, E, F) with increasing crustal heterogeneity. Model D was constructed by imposing a perturbation to the velocities at the specified knots of the interpolation, chosen from a uniform random distribution on ± 2 percent. After horizontal smoothing by averaging over 3 horizontal knots, the resulting perturbations in model D have about ±1 per cent heterogeneity in the crust with a horizontal scale length of about 100 km, and ±1 per cent heterogeneity has been introduced in the mantle as well. Models E and F retain the same mantle heterogeneity structure as model D but have higher

crustal heterogeneity amplitudes, in the initial perturbation stage up to ±5 per cent variation from the reference model was allowed for model E and ±10 per cent for model F. After horizontal smoothing, the variations from the reference model are of the order of ±2 per cent for model E and ±5 per cent for model F. We shall also consider model C with the same crustal structure as D, but no heterogeneity below the crust-mantle boundary.

After propagating a large horizontal distance in a heterogeneous model the energy originally in a single incident mode will no longer be confined to that mode, and indeed some energy may be reflected back by the heterogeneity, with again the possibility of conversion between modes. When the level of heterogeneity is relatively low (of the order of 1 per cent deviations from the stratified reference model - as in model D) transmission effects dominate and the level of reflected energy is negligible. Even with rather larger levels of heterogeneity the reflection from the whole model is small but, as pointed out by Maupin & Kennett (1987), it is necessary to retain apparently reflected waves in the course of the computation in order to get an accurate calculation of transmission effects. The Ricatti equations are much simpler when reflection can be neglected and so computation time can be reduced.

For any particular heterogeneous structure, it is therefore necessary to undertake a preliminary calculation including both reflection and transmission effects before it can be assumed that reflection can be ignored. The control of numerical accuracy in the course of the calculations is rather difficult, although for perfectly elastic models there is the possibility of monitoring the constancy of the total energy in reflection and transmission associated with an individual incident mode. To preserve full numerical precision quite small steps have to be taken in the horizontal direction: at 1.5 Hz the step should be no larger than 0.5 km if both reflected and transmitted waves are considered. For a number of models a somewhat larger step length gave reasonable results for the case of transmission alone.

The numerical calculations presented in this paper have been performed with the inclusion of both reflection and transmission effects, and energy conservation was satisfied to better than 0.25 per cent over 1000 km of propagation through heterogeneous structure. To reduce possible errors due to truncation of the modal sum, the calculations were carried out using a modal suite at least 5 modes larger than required by the truncation criterion. The reflection and transmission matrices for the full heterogeneous region were then truncated before display or other analysis.

For an incident mode at 0 km the effect of 1000 km of heterogeneity is that the energy originally in the mode is no longer confined to that particular mode. In figure 3 we show the transmission matrix for both Love and Rayleigh modes with the 22 mode set appropriate to the ARANDA reference model at 1.5 Hz, after passage through the heterogeneity model D. Each column of the matrix corresponds to the modal coefficients produced by the incidence of a single mode of amplitude 100 at 0 km. We see that the behaviour is dominated by the diagonal elements, but that significant mode conversions occur producing sizeable off-diagonal elements. For the Lg type modes (2-15) the bandwidth for significant interaction is typically ± 2 modes. The strong interaction of modes 2 and 3 arises because of their similar shape in the top 10 km. For the Sn modes (16-21), the eigenfunctions are very similar and there is strong interaction due to mantle perturbation extending to 200 km (the lower portion of the heterogeneity models are not shown in fig 2). However the separation from the Lg modes is striking; there is very little interaction except for modes 15 and 16 which share some of the characteristics of each group. The behaviour for Love and Rayleigh waves are similar, although they display some difference in their sensitivity to heterogeneity because the coupling terms in the Ricatti equations depend on different combinations of physical parameters.

As the frequency increases the number of modes need to cover the same phase velocity range increases, which causes some problems in combining the results from different frequencies. The increased size of the differential equation system also means an increase in computation time as the square of the number of modes if all mode interactions have to be considered. Fortunately, for the same model, the bandwidth of interaction increases only slowly with frequency. For Lg waves propagating through models similar to D with about 1 per cent heterogeneity, computations can be restricted to a band of 7 modes either side of the target mode without appreciable error for frequencies up to 2 Hz. At 1.5 Hz,

with 22 modes included, this bandwidth restriction has the effect of reducing computation time by nearly a factor of three.

The required bandwidth increases with the level of heterogeneity in the model (see figure 5). For model D in figure 2, a bandwidth of ±6 modes around the target mode is sufficient for both Lg and Sn modes. However to account for the interaction between modes for model E it is desirable to have at least a bandwidth of ±8 modes included in the calculation. For the highest level of heterogeneity illustrated in fig 2 (model F) a bandwidth of ±10 modes is definitely insufficient for full accuracy. For very heterogeneous models there is also the possibility of high angle propagation effects and so the size of the mode set has to be increased. Thus although the coupled mode approach is not confined to low level heterogeneity, the method is most effective when the structure does not deviate too far from the reference. A convenient working limit would seem to be about 2 per cent deviation as in model E.

In order to understand the effect of propagation through a heterogeneous model on the nature of regional phases we need to understand the characteristics of the surface wave modes in the reference model. In figure 4 we display the group slowness behaviour as a function of frequency up to 2 Hz for the first 40 Rayleigh modes on the ARANDA reference structure. The advantage of displaying the group slowness (the reciprocal of the group velocity) is that the various arrivals can be recognised in the time relationship that they have on a seismic record.

The Sn phase can be recognised in figure 4 as the superposition of many slowness maxima and minima at a slowness around 0.22 s/km (4.5 km/s). All 40 modes contribute to this tightly defined band of slownesses which clearly separates from the other classes of arrival. The onset of the Lg phase at a slowness of 0.286 s/km (3.5 km/s) is associated with the superposition of a number of relatively broad slowness minima arising from relatively low order modes. Following this onset is a more tangled skein of maxima and minima with slownesses less than 0.304 s/km (i.e. group velocities greater than 3.3 km/s), associated with about four modes at each frequency, which will provide the main Lg arrival. Somewhat later, we have a sequence of well defined slowness maxima associated with each mode in turn as the frequency increases. These maxima represent the Airy phase for each mode and will be significant contributors to the Lg coda; they arise physically from multiple reflections at angles to the vertical just greater than the critical angle for the crust-mantle boundary.

From the modal eigenfunction patterns displayed in figure 1, we can recognise that those modes (3-6) which contribute most to the onset of Lg at 1.5 Hz have the bulk of their energy confined to the middle and upper crust. The main Lg arrivals come from modes 7-10 which sample the whole crust. The Airy phases for modes 14, 15 arise just before the transition to energy transport in the mantle.

The effect of varying the heterogeneity level in the structural models can be well illustrated by comparing the energy distribution across the modal sequence for a single incident mode. In figure 5 we show this energy distribution for a set of incident modes at 0 km, at a frequency of 1.5 Hz, chosen to represent different parts of the Lg wave phase. We consider horizontal transmission through 1000 km of structure for four different models C, D, E and F with increasing levels of heterogeneity. Model C has 1 per cent of hetrogeneity confined to the crust. Models D, E and F are illustrated in figure 2, and have the same heterogeneity model in the mantle with about 1 per cent variation from the reference model (ARANDA, fig 1), but increasing levels of crustal heterogeneity (±1 per cent for D, ±2 per cent for E, and ±5 per cent for F).

At 1.5 Hz, mode 4 is a principal contributor to the onset of the Lg wave train. From fig 5a we see that for the incidence of this single mode at 0 km, the majority of the energy is carried in the original mode over the full 1000 km propagation path for the structures with up to 2 per cent variation away from the reference model (C,D,E). However, the proportion of energy in the original mode decreases as the crustal heterogeneity increases. As expected the mantle heterogeneity has very little influence on this group of interacting modes which is principally confined to the crust. Once we reach the highest level of heterogeneity (model F) the pattern of the energy distribution is markedly changed, the energy maximum is shifted over two modes to mode 6 which has a slightly different group velocity and energy is spread widely across the whole suite of crustal modes. There is very

little interaction with the fundamental or first higher modes because, as can be seen from figure 1, their energy is confined to the near surface and so is only sensitive to a small part of the total crustal heterogeneity.

For a mode in the main Lg wave arrivals (mode 9), we see from fig 5b that for the two models with relatively modest levels of heterogeneity (C,D) the energy is concentrated over three neighbouring modes centered on the incident mode. These three modes have group velocities varying by about 0.15 km/s and so the effect of the this level of heterogeneity will be to give a more diffuse maximum in the Lg wave amplitude. The presence of mantle heterogeneity now has a slight effect since it is possible to couple into modes with some energy penetration into the uppermost mantle. For the higher levels of crustal heterogeneity the incident energy gets spread out over a broader range of modes (6 are significant for model E and at least 10 for model F) and the effect on the Lg wavetrain will be more profound.

As a result of the dispersal of energy across a number of modes, for modest levels of heterogeneity (around 1 per cent), the best measure of Lg wave strength will be the integrated energy in a time window spanning group velocities of about 3.6-3.3 km/s for a typical continental situation; since the modes with these properties have their dominant interactions within the group.

Similar results arise for the Lg wave coda (incident mode 14) though this case, where the incident mode is most sensitive to lower crustal structure, is not as strongly affected by the heterogeneity as for mode 9. Even so, as we see in figure 5c, with increasing heterogeneity levels the representation of the propagation via the modes of the reference structure requires extensive mode coupling. For the higher heterogeneity levels there is significant energy shift into Sn type modes, which we can explain physically as occurring from local changes in the critical angle at the crust-mantle boundary. Modes like 14 travel close to the critical angle in the reference model and so a slight change of conditions can lead easily to energy transmission into the mantle, with a consequent shift of amplitude to modes like 17 and 18 (in the Sn suite). Energy is conserved across the whole modal field but is redistributed between the contributions of individual modes.

For incident modes 4 and 9, the nature of the energy spread induced across the modes of the reference structure has been principally to couple Lg type modes together and so the pattern of energy spread shows a skew towards higher mode numbers for mode 4 and lower numbers for mode 9. Whereas, for incident mode 14, the coupling is largely into a the immediate neighbouring modes with similar character and also into the Sn modes.

We should note that even for the moderately heterogeneous model D (fig 3) there has been a significant modification of the distribution of energy between modes after passage through 1000 km of structure. Such modifications over a band of frequencies will lead to theoretical seismograms which will differ significantly from the predictions for the horizontally stratified reference model.

We can simulate the effect of heterogeneity on theoretical seismograms, by modulating the modal coefficients by the appropriate transmission matrix. In order to reduce computational effort, whilst displaying a useful result, we have considered seismograms for a narrow frequency band and interpolated the modal transmission matrix between calculations for just a few frequencies. We restrict attention to explosive sources to simplify the source behaviour. In figure 6, we show seismograms at 1050 km for a source at 5km depth in the ARANDA model with a centre frequency of 1 Hz. The upper trace is for the horizontally stratified reference model and is dominated by Lg waves with relatively weak Sn. The two lower traces include the effect of transmission through 1000 km of the heterogeneous models D and E. The seismograms are normalised to the same peak amplitude and relative amplitudes are indicated to the right of figure 6. The behaviour of these theoretical seismograms illustrates clearly the character of the intermode interactions we have already discussed. The ARANDA model has a weak gradient for S velocity in the mantle and so the Sn phase is relatively weak for the horizontally stratified model. However the coupling between the Lg and Sn wavegudes induced by the heterogeneity leads to an increase in Sn amplitude, principally at the expense of the Lg coda. Whilst model D with only 1 per cent hetrogeneity shows most change in the onset of Lg, the higher level of heterogeneity in model E has lead to a smearing out of the most energetic part of the Lg phase with an amplitude reduction of about 10 per cent. The Lg wavetrain

-44-

can be viewed either as a superposition of many multiple reflections within the crustal waveguide or as a interference of many modes. The effect of heterogeneity is to change the relative arrival times of the multiple reflections and thus the phases of the different modes so that the interfence pattern changes. Because there is a delicate balance between constructive and destructive interference, relatively small changes in timing can have a substantial effect on the waveform.

These results show that propagation over hundreds of kilometres through structures with relatively long wavelength of heterogeneity can have substantial effect on the character of the Lg wave train. However, in addition to large scale effects, there is abundant evidence for small scale heterogeneity on a scale of tens of kilometres with amplitudes of a few percent (see e.g. Aki 1981). We need to know what is the effect of such small scale heterogeneity and how it may affect long range propagation.

Small scale heterogeneity

In order to look at concentrated local heterogeneity we have considered the effects of the same velocity perturbations as before but on a compressed distance scale. We have taken the same velocity values as in models D and E above (fig 2) but reduced the horizontal scale by a factor of 10 so that in the new models H (approximately ±1 per cent variation) and I (approximately ± 2 per cent) the heterogeneity is concentrated in a 100 km zone. The velocity sampling is now at 4km horizontal intervals. This yields velocity perturbations of a few percent with a horizontal heterogeneity scale of around 10 km, representing the smaller scale features commonly found in the crust.

For these scales of heterogeneity, as frequency increases and consequently wavelength diminishes, the size of the off-diagonal elements in the modal coupling matrix increase at the expense of the diagonal elements which will induce a broader spread in the group slownesses associated with the propagation.

The heterogeneity model H has relatively little effect on the modes: there is a spread of energy away from the incident mode after a 100 km passage through the model, but this is principally to nearest neighbour modes which will, in general, have similar character. Once the heterogeneity level increases (to around ± 2 per cent in model I) the behaviour is not so simple . The transmission matrix is still diagonal dominated but there is now coupling over a span of a number of modes. These effects can be illustrated well by once again forming theoretical seismograms with a narrow frequency band. To allow direct comparison with figure 6 we have once again considered the seismograms at a distance of 1050 km with a centre frequency of 1 Hz.

In figure 7 we show the theoretical seismograms at 1050 km including the effect of passage through 100 km of small scale heterogeneity; the upper trace is for the horizontally stratified reference model. For model H (± 1 per cent) the difference in waveform is slight and can only be seen on careful inspection but the amplitude has decreased by nearly 5 per cent. However, with ± 2 per cent heterogeneity as in model I there is a noticeable change in waveform and a small, but significant, transfer of energy ahead of the main Lg phase. The amplitude maximum is now more sharply defined and large than in the absence of heterogeneity due to favourable constructive interference. The coupling between modes is at its strongest for the lower orders and this is reflected by the change in the nature of the onset of Lg. Thus, a substantial change in the character of the Lg wavetrain can be produced by only 100 km of moderate, small-scale, heterogeneity. So that it is clear that the cumulative effect of multiple scattering within the crust can be substantial and that observed waveforms can be heavily shaped by the propagation path as well as the source characteristics (even in the absence of major lateral heterogeneity).

DISCUSSION

The results of the studies of Lg wave propagation in heterogeneous models for the crust and upper mantle show that reflection from distributed heterogeneity is not very important. However, both reflection and transmission processes should be included, if at all possible, in the numerical calculations in order to ensure the accuracy of estimates of modal transmission. The coupled mode technique works well with heterogeneous models which differ from a stratified reference model by up to 2 per cent with a limited bandwidth

of interaction between modes. The approach can be used for higher levels of heterogeneity but a large number of modes need to be considered with consequent high computation costs.

One of the major effects of crustal heterogeneity is to introduce the possibility of smearing out the main amplitude peak in the Lg wave train over a band of group velocities. As a result, an effective measure of the energy content of the Lg waves will be to consider the integrated amplitude along the traces beween group velocities of 3.6 and 3.3 km/s. The influence of mantle heterogeneity on Lg wave propagation was found to be quite small. However, any conversion into Sn type modes will give arrivals which will have apparent group velocities of between 4.3 and 3.7 km/s, depending on the position where conversion occurs. Such arrivals will appear in a portion of the seismic record which would be predicted to be very quiet in stratified medium calculations, and as a result may appear to be more prominent than expected. The increase of energy in this time interval for the heterogeneous models goes some way towards reconciling theoretical seismograms with the character of observed regional phases.

ACKNOWLEDGEMENTS

REFERENCES

Aki K. (1981) Attenuation and scattering of short period seismic waves in the lithosphere, in *Identification of Seismic Sources - Earthquake or Underground Explosion* ed E.S. Husebye & S. Mykkeltveit, Noordhof, Leiden

Kennett B.L.N. (1984) Guided wave propagation in laterally varying media - I. Theoretical development, *Geophys J R astr Soc* , 79, 235-255

Kennett B.L.N. & Mykkeltveit S. (1984) Guided wave propagation in laterally varying media - II Lg wave in northwestern Europe, *Geophys J R astr Soc*, 79, 257-267

Maupin V. & Kennett B.L.N. (1987) On the use of truncated modal expansions in laterally varying media, *Geophys J R astr Soc*, 91, 837-851

Pomeroy P.W., Best W.J. & McEvilly T.V. (1982) Test ban treaty verification with regional data a review, *Bull. Seism. Soc. Am.*, 72, S89-S129
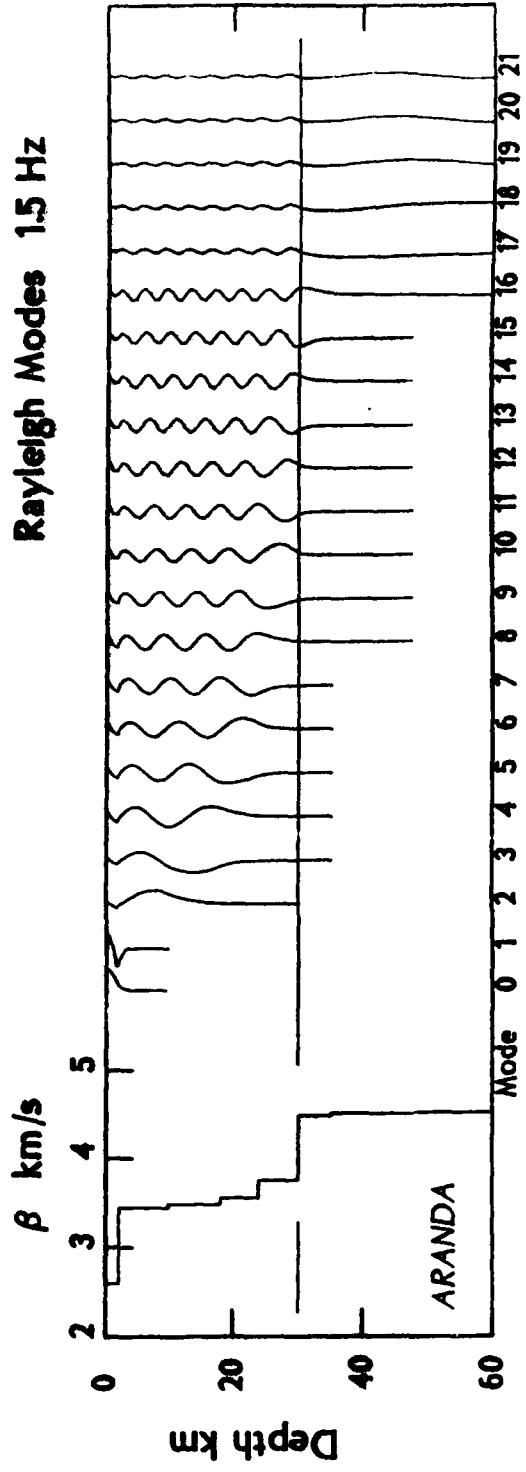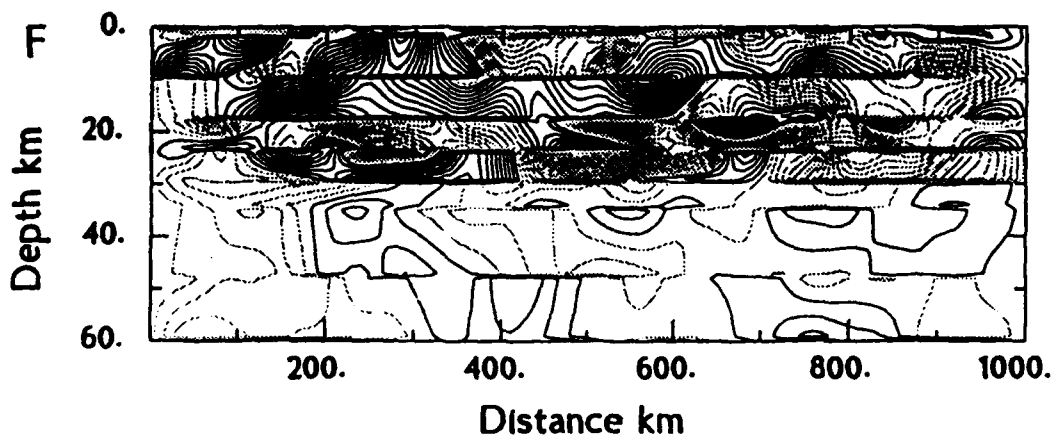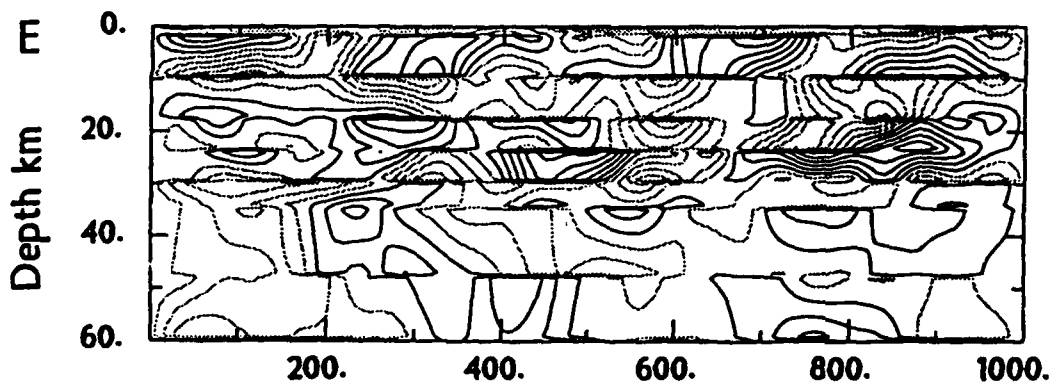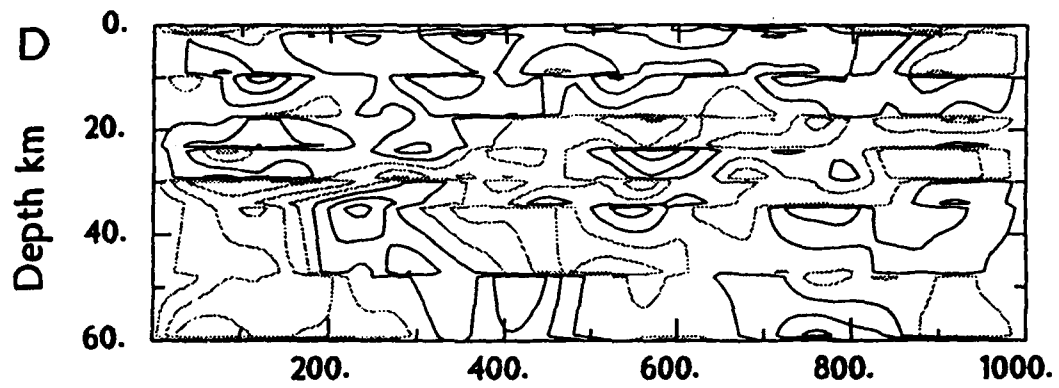
FIGURE CAPTIONS

Figure 1: ARANDA reference model with Love and Rayleigh mode eigenfunctions for phase velocity less than 4.54 km/s, at frequency 1.5 Hz.

Figure 2: Contour plots of the sequence of heterogeneous velocity models used in the studies of Lg wave propagation. The heavier lines indicate positive perturbations away from the ARANDA reference model, and the contour interval is 0.5 per cent perturbation.

Figure 3: Representation of the transmission matrix for Love and Rayleigh modes at 1.5 Hz after passage through 1000 km of model D. Amplitude values less than 1 are left blank.

Figure 4: Group slowness beviour as a function of frequency for the first 40 Rayleigh modes of the ARANDA reference model illustrated in figure 1.

Figure 5: Energy distribution across the Love and Rayleigh modes for the ARANDA reference model at 1.5 Hz, after transmission through 1000 km of heterogeneous structure. The symbols denote the different hetrogeneity models, as discussed in the text: a) incident mode 4, b) incident mode 9, c) incident mode 14.

Figure 6: Theoretical seismograms at 1050 km for a narrow frequency band around 1 Hz illustrating the effect of broad scale heterogeneity on the regional S wavetrain. The upper trace is for the horizontally stratified ARANDA reference model and the two lower traces for propagation through 1000 km of heterogeneity models D ($\pm$ 1 per cent) and E ($\pm$ 2 per cent). The seismograms are normalised to the same peak amplitude and the relative amplitudes are indicated to the right of each seismogram.
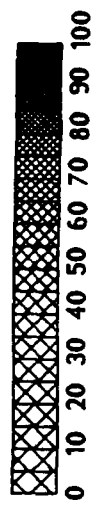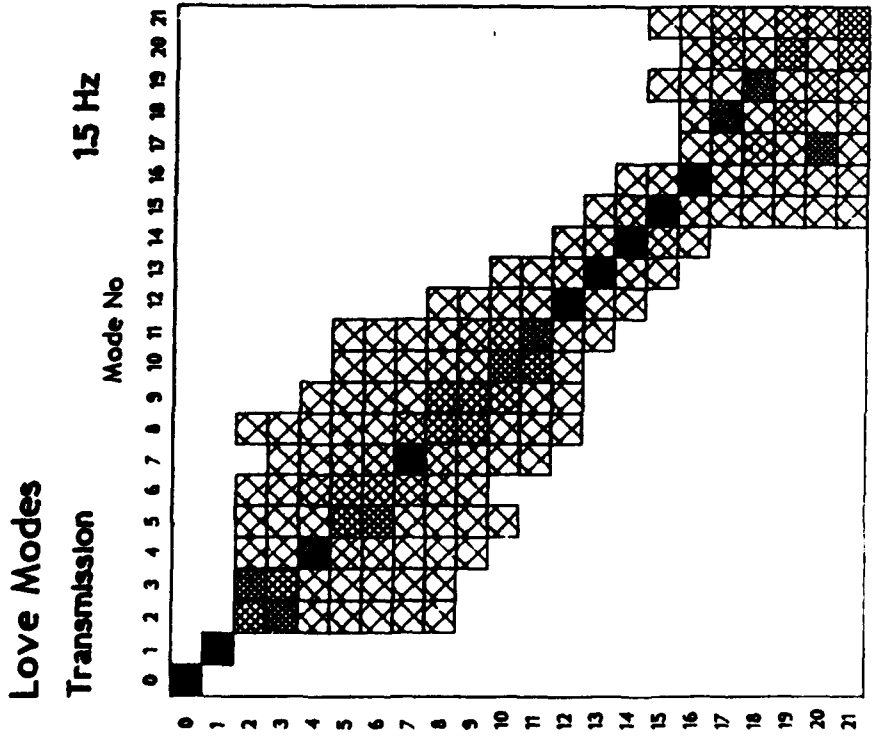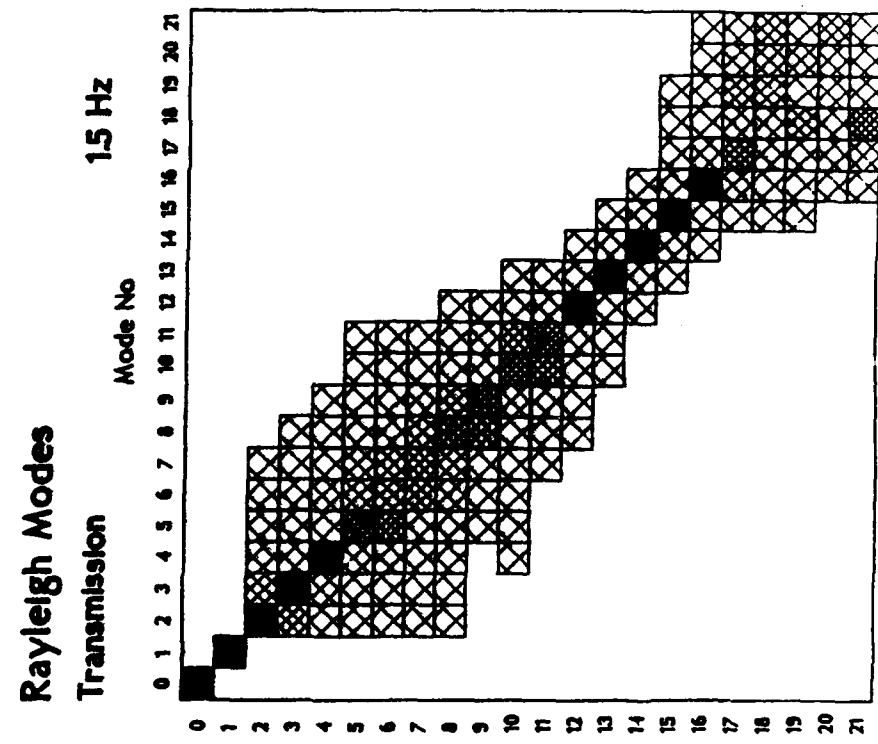
Figure 7: Theoretical seismograms at 1050 km for a narrow frequency band around 1 Hz illustrating the effect of small scale heterogeneity on the regional S wavetrain. The upper trace is for the horizontally stratified ARANDA reference model and the two lower traces for propagation through 100km of heterogeneity models H ($\pm$ 1 per cent) and I ($\pm$ 2 per cent). The seismograms are normalised to the same peak amplitude and the relative amplitudes are indicated to the right of each seismogram.
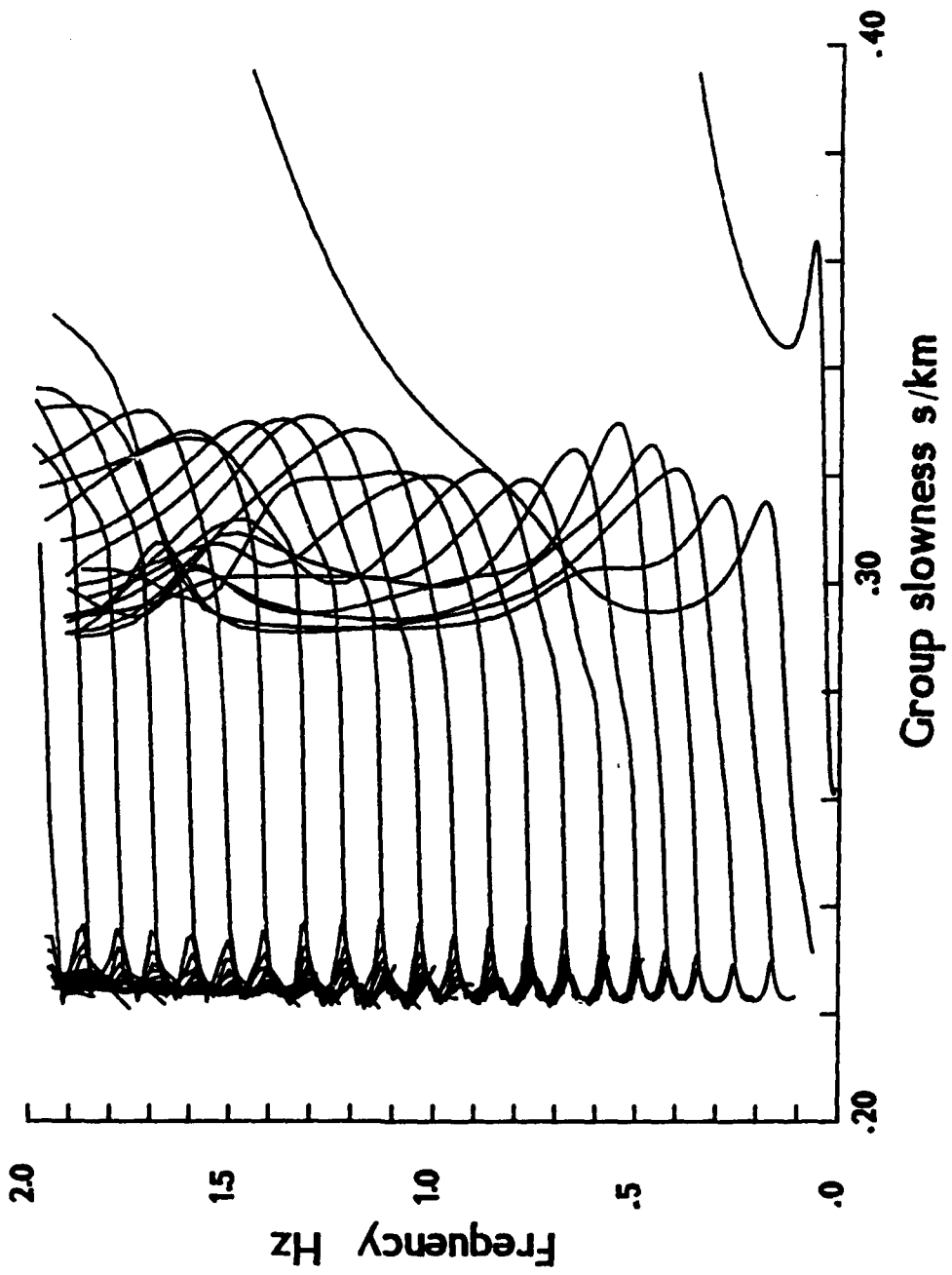
Love Modes 1.5 Hz

Rayleigh Modes 1.5 Hz

Love Modes

Rayleigh Modes

a Love Modes   Incident Mode 4   Rayleigh Modes   Incident Mode 4

b Love Modes   Incident Mode 9   Rayleigh Modes   Incident Mode 9

c Love Modes   Incident Mode 14   Rayleigh Modes   Incident Mode 14
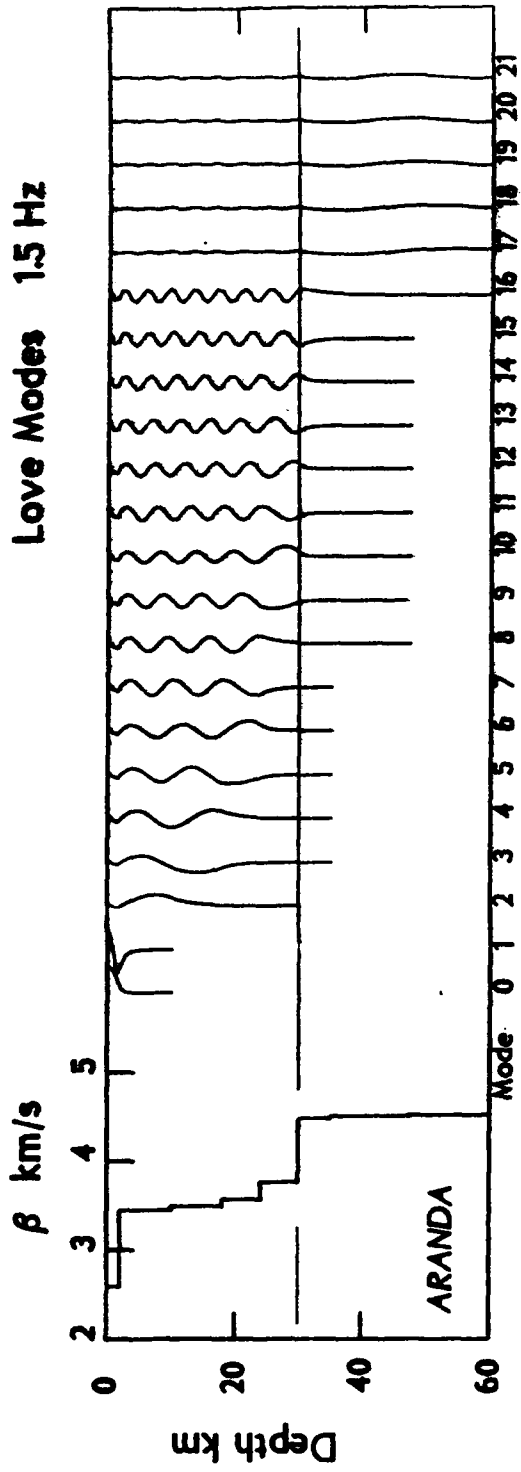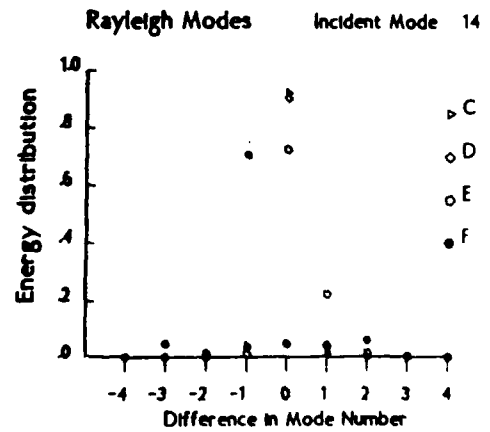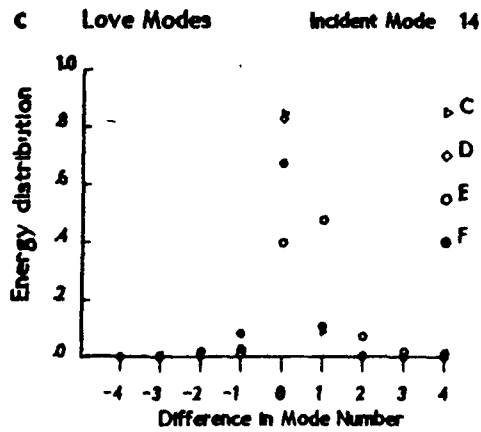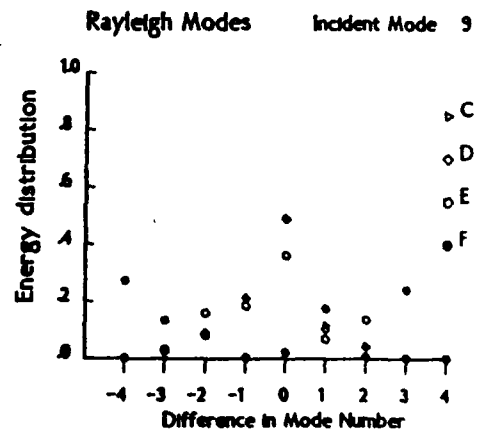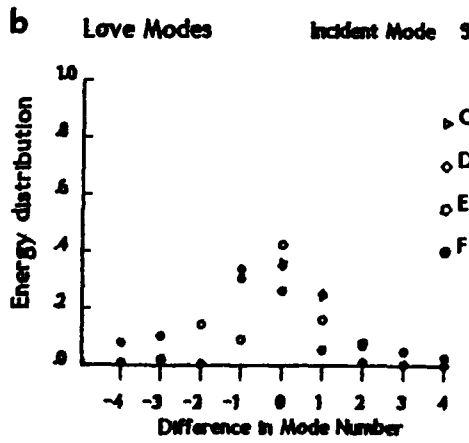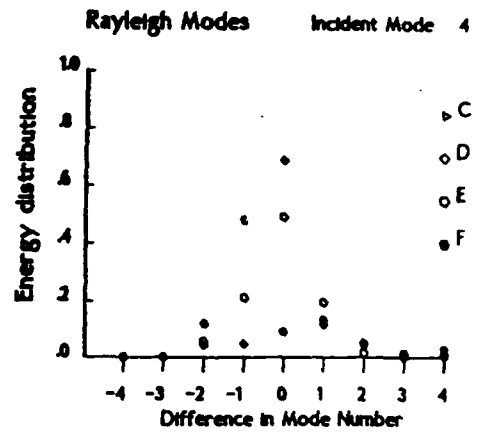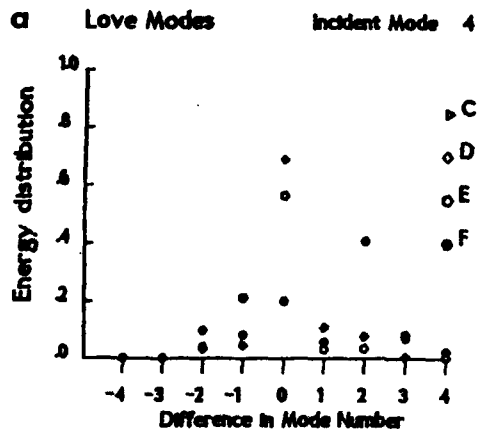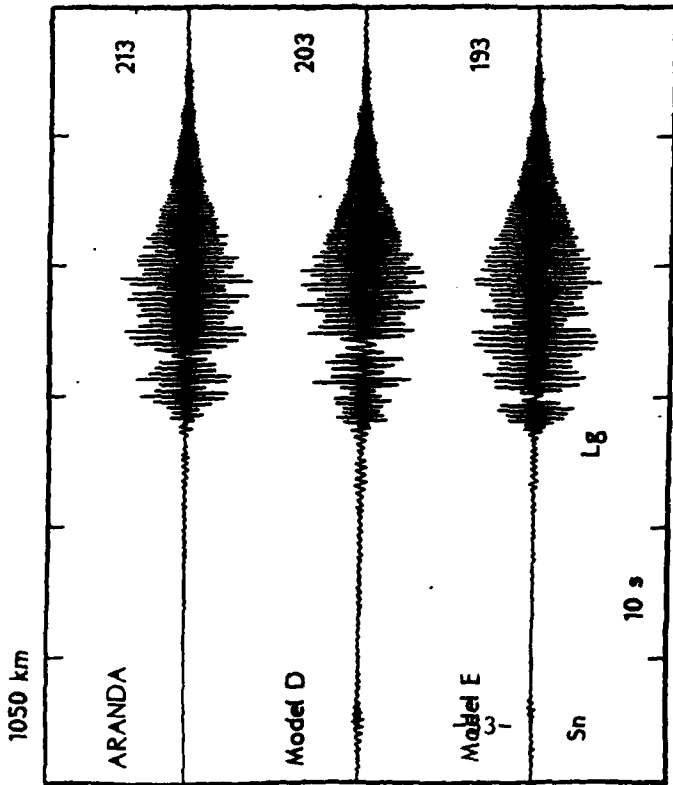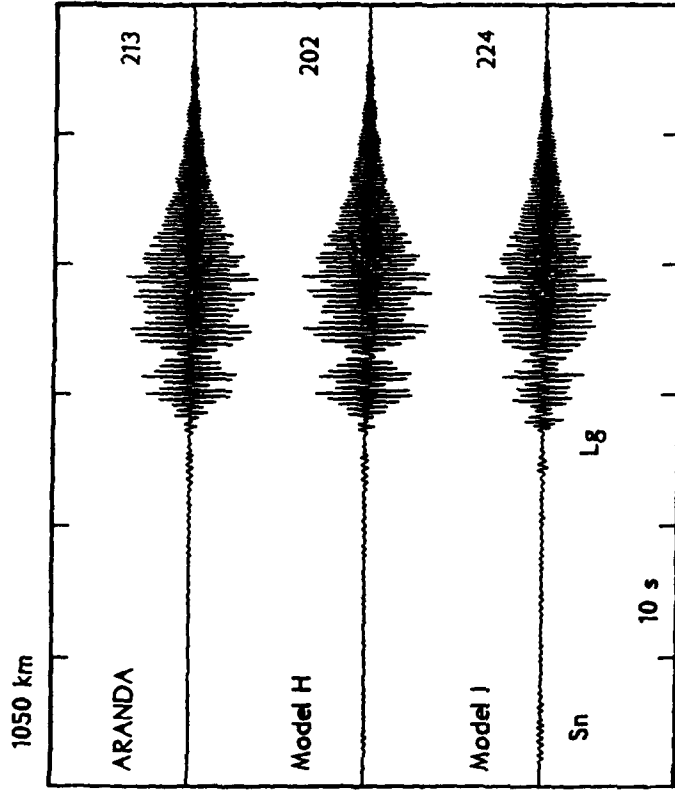
DISTRIBUTION OF RESEARCH RESULTS

a) PUBLICATIONS

Kennett B.L.N. (1989a) On the nature of regional seismic phases I -
  phase representations for Pn, Pg, Sn and Lg.
  Geophys. J. in press

Kennett B.L.N. (1989b) Lg wave propagation in heterogeneous media,
  Bull. seism. Soc. Am. in press

b) PRESENTATIONS

On representing surface wave propagation in laterally varying media by
truncated modal expansions
  DARPA/AFGL Seismic Research Symposium
  Nantucket, Massachusetts, June 1987

Coupled wavenumber methods for guided waves in heterogeneous media
  DARPA/AFGL Seismic Research Symposium
  Fallbrook, California, May 1988

Guided waves in laterally heterogeneous media
  Seminar, Hawaii Institute of Geophysics, August 1987
  Seminar, Center for Seismic Studies, May 1988
  Seminar, Norwegian Seismic Array, June 1988

Regional seismic phases in seismic discrimination
  Seminar, Research School of Earth Sciences, Australian National
  University, November 1988

CONTRACTORS (United States)

Professor Keiiti Aki
Center for Earth Sciences
University of Southern California
University Park
Los Angeles, CA 90089-0741

Professor Thomas Ahrens
Seismological Lab, 252-21
Div. of Geological and Planetary
  Sciences
California Institute of Technology
Pasadena, CA 91125

Professor Charles B. Archambeau
Cooperative Institute for Resch
  in Environmental Sciences
University of Colorado
Boulder, CO 80309

Dr. Thomas C. Bache Jr.
Science Applications Int'l Corp.
10210 Campus Point Drive
San Diego, CA 92121   (2 copies)

Dr. Muawia Barazangi
Institute for the Study of
  of the Continent
Cornell University
Ithaca, NY 14853

Dr. Douglas R. Baumgardt
Signal Analysis & Systems Div.
ENSCO, Inc.
5400 Port Royal Road
Springfield, VA 22151-2388

Dr. Jonathan Berger
Institute of Geophysics and
  Planetary Physics
Scripps Institution of Oceanography
A-025
University of California, San Diego
La Jolla, CA 92093

Dr. S. Bratt
Science Applications Int'l Corp.
10210 Campus Point Drive
San Diego, CA 92121

Dr. Lawrence J. Burdick
Woodward-Clyde Consultants
P.O. Box 93245
Pasadena, CA 91109-3245 (2 copies)

Professor Robert W. Clayton
Seismological Laboratory/Div. of
  Geological & Planetary Sciences
California Institute of Technology
Pasadena, CA 91125

Dr Karl Coyner
New England Research, Inc.
76 Olcott Drive
White River Junction, VT 05001

Dr. Vernon F. Cormier
Department of Geology & Geophysics
U-45, Room 207
The University of Conneticut
Storrs, Connecticut 06268

Dr. Steven Day
Dept. of Geological Sciences
San Diego State U.
San Diego, CA 92182

Dr. Zoltan A. Der
ENSCO, Inc.
5400 Port Royal Road
Springfield, VA 22151-2388

Professor John Ferguson
Center for Lithospheric Studies
The University of Texas at Dallas
P.O. Box 830688
Richardson, TX 75083-0688

Professor Stanley Flatte'
Applied Sciences Building
University of California,
Santa Cruz, CA 95064

Dr. Alexander Florence
SRI International
333 Ravenswood Avenue
Menlo Park, CA 94025-3493

Professor Steven Grand
University of Texas at Austin
Dept of Geological Sciences
Austin, TX 78713-7909

Dr. Henry L. Gray
Associate Dean of Dedman College
Department of Statistical Sciences
Southern Methodist University
Dallas, TX 75275

Professor Roy Greenfield
Geosciences Department
403 Deike Building
The Pennsylvania State University
University Park, PA 16802

Professor David G. Harkrider
Seismological Laboratory
Div of Geological & Planetary Sciences
California Institute of Technology
Pasadena, CA 91125

Professor Donald V. Helmberger
Seismological Laboratory
Div of Geological & Planetary Sciences
California Institute of Technology
Pasadena, CA 91125

Professor Eugene Herrin
Institute for the Study of Earth
   and Man/Geophysical Laboratory
Southern Methodist University
Dallas, TX 75275

Professor Robert B. Herrmann
Department of Earth & Atmospheric
      Sciences
Saint Louis University
Saint Louis, MO 63156

Professor Bryan Isacks
Cornell University
Dept of Geological Sciences
SNEE Hall
Ithaca, NY 14850

Professor Lane R. Johnson
Seismographic Station
University of California
Berkeley, CA 94720

Professor Thomas H. Jordan
Department of Earth, Atmospheric
 and Planetary Sciences
Mass Institute of Technology
Cambridge, MA 02139

Dr. Alan Kafka
Department of Geology &
   Geophysics
Boston College
Chestnut Hill, MA 02167

Professor Leon Knopoff
University of California
Institute of Geophysics
   & Planetary Physics
Los Angeles, CA 90024

Professor Charles A. Langston
Geosciences Department
403 Deike Building
The Pennsylvania State University
University Park, PA 16802

Professor Thorne Lay
Department of Geological Sciences
1006 C.C. Little Building
University of Michigan
Ann Arbor, MI 48109-1063

Dr. Randolph Martin III
New England Research, Inc.
76 Olcott Drive
White River Junction, VT 05001

Dr. Gary McCartor
Mission Research Corp.
735 State Street
P.O. Drawer 719
Santa Barbara, CA 93102   (2 copies)

Professor Thomas V. McEvilly
Seismographic Station
University of California
Berkeley, CA 94720

Dr. Keith L. McLaughlin
S-CUBED,
A Division of Maxwell Laboratory
P.O. Box 1620
La Jolla, CA 92038-1620

Professor William Menke
Lamont-Doherty Geological Observatory
   of Columbia University
Palisades, NY 10964

Professor Brian J. Mitchell
Department of Earth & Atmospheric
   Sciences
Saint Louis University
Saint Louis, MO 63156

Mr. Jack Murphy
S-CUBED
A Division of Maxwell Laboratory
11800 Sunrise Valley Drive
Suite 1212
Reston, VA 22091 (2 copies)

Professor J. A. Orcutt
IGPP, A-205
Scripps Institute of Oceanography
Univ. of California, San Diego
La Jolla, CA 92093

Professor Keith Priestley
University of Nevada
Mackay School of Mines
Reno, NV 89557

Professor Paul G. Richards
Lamont-Doherty Geological
Observatory of Columbia Univ.
Palisades, NY 10964

Wilmer Rivers
Teledyne Geotech
314 Montgomery Street
Alexandria, VA 22314

Dr. Alan S. Ryall, Jr.
Center of Seismic Studies
1300 North 17th Street
Suite 1450
Arlington, VA 22209-2308   (4 copies)

Professor Charles G. Sammis
Center for Earth Sciences
University of Southern California
University Park
Los Angeles, CA 90089-0741

Professor Christopher H. Scholz
Geological Sciences
Lamont-Doherty Geological Observatory
Palisades, NY 10964

Dr. Jeffrey L. Stevens
S-CUBED,
A Division of Maxwell Laboratory
P.O. Box 1620
La Jolla, CA 92038-1620

Professor Brian Stump
Institute for the Study of Earth & Man
Geophysical Laboratory
Southern Methodist University
Dallas, TX 75275

Professor Ta-liang Teng
Center for Earth Sciences
University of Southern California
University Park
Los Angeles, CA 90089-0741

Dr. Clifford Thurber
State University of New York at
  Stony Brooks
Dept of Earth and Space Sciences
Stony Brook, NY 11794-2100

Professor M. Nafi Toksoz
Earth Resources Lab
Dept of Earth, Atmospheric and
  Planetary Sciences
Massachusetts Institute of Technology
42 Carleton Street
Cambridge, MA 02142

Professor Terry C. Wallace
Department of Geosciences
Building #77
University of Arizona
Tucson, AZ 85721

Weidlinger Associates
ATTN: Dr. Gregory Wojcik
4410 El Camino Real, Suite 110
Los Altos, CA 94022

Professor Francis T. Wu
Department of Geological Sciences
State University of New York
  at Binghamton
Vestal, NY 13901

Dr. Monem Abdel-Gawad
Rockwell Internat'l Science Center
1049 Camino Dos Rios
Thousand Oaks, CA 91360

Professor Shelton S. Alexander
Geosciences Department
403 Deike Building
The Pennsylvania State University
University Park, PA 16802

Dr. Ralph Archuleta
Department of Geological
  Sciences
Univ. of California at
  Santa Barbara
Santa Barbara, CA

J. Barker
Department of Geological Sciences
State University of New York
  at Binghamton
Vestal, NY   13901

Mr. William J. Best
907 Westwood Drive
Vienna, VA   22180

Dr. N. Biswas
Geophysical Institute
University of Alaska
Fairbanks, AK 99701

Dr. G. A. Bollinger
Department of Geological Sciences
Virginia Polytechnical Institute
21044 Derring Hall
Blacksburg, VA   24061

Mr. Roy Burger
1221 Serry Rd.
Schenectady, NY   12309

Dr. Robert Burridge
Schlumberger-Doll Resch Ctr.
Old Quarry Road
Ridgefield, CT   06877

Science Horizons, Inc.
ATTN: Dr. Theodore Cherry
710 Encinitas Blvd., Suite 101
Encinitas, CA   92024   (2 copies)

Professor Jon F. Claerbout
Professor Amos Nur
Dept. of Geophysics
Stanford University
Stanford, CA   94305 (2 copies)

Dr. Anton W. Dainty
AFGL/LWH
Hanscom AFB, MA   01731

Professor Adam Dziewonski
Hoffman Laboratory
Harvard University
20 Oxford St.
Cambridge, MA   02138

Professor John Ebel
Dept of Geology and Geophysics
Boston College
Chestnut Hill, MA   02167

Dr. Donald Forsyth
Dept of Geological Sciences
Brown University
Providence, RI   02912

Dr. Anthony Gangi
Texas A&M University
Department of Geophysics
College Station, TX   77843

Dr. Freeman Gilbert
Institute of Geophysics &
  Planetary Physics
University of California, San Diego
P.O. Box 109
La Jolla, CA   92037

Mr. Edward Giller
Pacific Seirra Research Corp.
1401 Wilson Boulevard
Arlington, VA   22209

Dr. Jeffrey W. Given
Sierra Geophysics
11255 Kirkland Way
Kirkland, WA 98033

Rong Song Jih
Teledyne Geotech
314 Montgomery Street
Alexandria, Virginia 22314

Professor F.K. Lamb
University of Illinois at
    Urbana-Champaign
Department of Physics
1110 West Green Street
Urbana, IL 61801

Dr. Arthur Lerner-Lam
Lamont-Doherty Geological Observatory
 of Columbia University
Palisades, NY 10964

Dr. L. Timothy Long
School of Geophysical Sciences
Georgia Institute of Technology
Atlanta, GA 30332

Dr. Peter Malin
University of California at
    Santa Barbara
Institute for Central Studies
Santa Barbara, CA 93106

Dr. George R. Mellman
Sierra Geophysics
11255 Kirkland Way
Kirkland, WA 98033

Dr. Bernard Minster
IGPP, A-205
Scripps Institute of Oceanography
Univ. of California, San Diego
La Jolla, CA 92093

Professor John Nabelek
College of Oceanography
Oregon State University
Corvallis, OR 97331

Dr. Geza Nagy
U. California, San Diego
Dept of Ames, M.S. B-010
La Jolla, CA 92093

Dr. Jack Oliver
Department of Geology
Cornell University
Ithaca, NY 14850

Dr. Robert Phinney/Dr. F. A. Dahlen
Dept of Geological
Geological Science University
Princeton University
Princeton, NJ 08540

RADIX System, Inc.
Attn: Dr. Jay Pulli
2 Taft Court, Suite 203
Rockville, Maryland 20850

Dr. Norton Rimer
S-CUBED
A Division of Maxwell Laboratory
P.O. 1620
La Jolla, CA 92038-1620

Professor Larry J. Ruff
Department of Geological Sciences
1006 C.C. Little Building
University of Michigan
Ann Arbor, MI 48109-1063

Dr. Richard Sailor
TASC Inc.
55 Walkers Brook Drive
Reading, MA 01867

Thomas J. Sereno, Jr.
Service Application Int'l Corp.
10210 Campus Point Drive
San Diego, CA 92121

Dr. David G. Simpson
Lamont-Doherty Geological Observ.
 of Columbia University
Palisades, NY 10964

Dr. Bob Smith
Department of Geophysics
University of Utah
1400 East 2nd South
Salt Lake City, UT 84112

Dr. S. W. Smith
Geophysics Program
University of Washington
Seattle, WA 98195

Dr. Stewart Smith
IRIS Inc.
1616 N. Fort Myer Drive
Suite 1440
Arlington, VA 22209

Rondout Associates
ATTN: Dr. George Sutton,
Dr. Jerry Carter, Dr. Paul Pomeroy
P.O. Box 224
Stone Ridge, NY 12484 (4 copies)

Dr. L. Sykes
Lamont Doherty Geological Observ.
Columbia University
Palisades, NY 10964

Dr. Pradeep Talwani
Department of Geological Sciences
University of South Carolina
Columbia, SC 29208

Dr. R. B. Tittmann
Rockwell International Science Center
1049 Camino Dos Rios
P.O. Box 1085
Thousand Oaks, CA 91360

Professor John H. Woodhouse
Hoffman Laboratory
Harvard University
20 Oxford St.
Cambridge, MA 02138

Dr. Gregory B. Young
ENSCO, Inc.
5400 Port Royal Road
Springfield, VA 22151-2388

Dr. Peter Basnam
Earth Physics Branch
Geological Survey of Canada
1 Observatory Crescent
Ottawa, Ontario
CANADA KIA OY3

Professor Ari Ben-Menahem
Dept of Applied Mathematics
Weizman Institute of Science
Rehovot
ISRAEL 951729

Dr. Eduard Berg
Institute of Geophysics
University of Hawaii
Honolulu, HI 96822

Dr. Michel Bouchon - Universite
   Scientifique et Medicale de Grenob
Lab de Geophysique - Interne et
   Tectonophysique - I.R.I.G.M-B.P.
38402 St. Martin O'Heres
Cedex FRANCE

Dr. Hilmar Bungum/NTNF/NORSAR
P.O. Box 51
Norwegian Council of Science,
Industry and Research, NORSAR
N-2007 Kjeller, NORWAY

Dr. Michel Campillo
I.R.I.G.M.-B.P. 68
38402 St. Martin O'Heres
Cedex, FRANCE

Dr. Kin-Yip Chun
Geophysics Division
Physics Department
University of Toronto
Ontario, CANADA M5S 1A7

Dr. Alan Douglas
Ministry of Defense
Blacknest, Brimpton,
 Reading RG7-4RS
UNITED KINGDOM

Dr. Manfred Henger
Fed. Inst. For Geosciences & Nat'l Res.
Postfach 510153
D-3000 Hannover 51
FEDERAL REPUBLIC OF GERMANY

Ms. Eva Johannisson
Senior Research Officer
National Defense Research Inst.
P.O. Box 27322
S-102 54 Stockholm
SWEDEN

Tormod Kvaerna
NTNF/NORSAR
P.O. Box 51
N-2007 Kjeller, NORWAY

Mr. Peter Marshall, Procurement
 Executive, Ministry of Defense
Blacknest, Brimpton,
 Reading FG7-4RS
UNITED KINGDOM (3 copies)

Dr. Robert North
Geophysics Division
Geological Survey of Canada
1 Observatory crescent
Ottawa, Ontario
CANADA, KIA OY3

Dr. Frode Ringdal
NTNF/NORSAR
P.O. Box 51
N-2007 Kjeller, NORWAY

Dr. Jorg Schlittenhardt
Federal Inst. for Geosciences & Nat'l Res.
Postfach 510153
D-3000 Hannover 51
FEDERAL REPUBLIC OF GERMANY

University of Hawaii
Institute of Geophysics
ATTN: Dr. Daniel Walker
Honolulu, HI 96822

Dr. Ramon Cabre, S.J.
Observatorio San Calixto
Casilla 5939
La Paz Bolivia

Professor Peter Harjes
Institute for Geophysik
Rhur University/Bochum
P.O. Box 102148, 4630 Bochum 1
FEDERAL REPUBLIC OF GERMANY

Dr. E. Husebye
NTNF/NORSAR
P.O. Box 51
N-2007 Kjeller, NORWAY

Professor Brian L.N. Kennett
Research School of Earth Sciences
Institute of Advanced Studies
G.P.O. Box 4
Canberra 2601
AUSTRALIA

Dr. B. Massinon
Societe Radiomana
27, Rue Claude Bernard
7,005, Paris, FRANCE   (2 copies)

Dr. Pierre Mechler
Societe Radiomana
27, Rue Claude Bernard
75005, Paris, FRANCE

Dr. Svein Mykkeltveit
NTNF/NORSAR
P.O. Box 51
N-2007 Kjeller, NORWAY   (3 copies)

Dr. Ralph Alewine III
DARPA/NMRO
1400 Wilson Boulevard
Arlington, VA 22209-2308

Dr. Robert Blandford
DARPA/NMRO
1400 Wilson Boulevard
Arlington, VA 22209-2308

Sandia National Laboratory
ATTN: Dr. H. B. Durham
Albuquerque, NM 87185

Dr. Jack Evernden
USGS-Earthquake Studies
345 Middlefield Road
Menlo Park, CA 94025

U.S. Geological Survey
ATTN: Dr. T. Hanks
Nat'l Earthquake Resch Center
345 Middlefield Road
Menlo Park, CA 94025

Dr. James Hannon
Lawrence Livermore Nat'l Lab.
P.O. Box 808
Livermore, CA 94550

Paul Johnson
ESS-4, Mail Stop J979
Los Alamos National Laboratory
Los Alamos, NM 87545

Ms. Ann Kerr
DARPA/NMRO
1400 Wilson Boulevard
Arlington, VA 22209-2308

Dr. Max Koontz
US Dept of Energy/DP 5
Forrestal Building
1000 Independence Ave.
Washington, D.C. 20585

Dr. W. H. K. Lee
USGS
Office of Earthquakes, Volcanoes,
  & Engineering
Branch of Seismology
345 Middlefield Rd
Menlo Park, CA 94025

Dr. William Leith
U.S. Geological Survey
Mail Stop 928
Reston, VA 22092

Dr. Richard Lewis
Dir. Earthquake Engineering and
  Geophysics
U.S. Army Corps of Engineers
Box 631
Vicksburg, MS 39180

Dr. Robert Masse'
Box 25046, Mail Stop 967
Denver Federal Center
Denver, Colorado 80225

Richard Morrow
ACDA/VI
Room 5741
320 21st Street N.W.
Washington, D.C. 20451

Dr. Keith K. Nakanishi
Lawrence Livermore National Laboratory
P.O. Box 808, L-205
Livermore, CA 94550 (2 copies)

Dr. Carl Newton
Los Alamos National Lab.
P.O. Box 1663
Mail Stop C335, Group ESS-3
Los Alamos, NM 87545

Dr. Kenneth H. Olsen
Los Alamos Scientific Lab.
P.O. Box 1663
Mail Stop C335, Group ESS-3
Los Alamos, NM 87545

Howard J. Patton
Lawrence Livermore National
  Laboratory
P.O. Box 808, L-205
Livermore, CA 94550

Mr. Chris Paine
Office of Senator Kennedy
SR 315
United States Senate
Washington, D.C. 20510

AFOSR/NP
ATTN: Colonel Jerry J. Perrizo
Bldg 410
Bolling AFB, Wash D.C. 20332-6448

HQ AFTAC/TT
Attn: Dr. Frank F. Pilotte
Patrick AFB, Florida 32925-6001

Mr. Jack Rachlin
USGS - Geology, Rm 3 C136
Mail Stop 928 National Center
Reston, VA 22092

Robert Reinke
AFWL/NTESG
Kirtland AFB, NM 87117-6008

Dr. Byron Ristvet
HQ DNA, Nevada Operations Office
Attn: NVCG
P.O. Box 98539
Las Vegas, NV 89193

HQ AFTAC/TGR
Attn: Dr. George H. Rothe
Patrick AFB, Florida 32925-6001

Donald L. Springer
Lawrence Livermore National Laboratory
P.O. Box 808, L-205
Livermore, CA 94550

Dr. Lawrence Turnbull
OSWR/NED
Central Intelligence Agency
CIA, Room 5G48
Washington, D.C. 20505

Dr. Thomas Weaver
Los Alamos National Laboratory
P.O. Box 1663
MS C 335
Los Alamos, NM 87545

GL/SULL
Research Library
Hanscom AFB, MA 01731-5000 (2 copies)

Secretary of the Air Force (SAFRD)
Washington, DC 20330
Office of the Secretary Defense
DDR & E
Washington, DC 20330

HQ DNA
ATTN: Technical Library
Washington, DC 20305

DARPA/RMO/RETRIEVAL
1400 Wilson Blvd.
Arlington, VA 22209

DARPA/RMO/Security Office
1400 Wilson Blvd.
Arlington, VA 22209

GL/XO
Hanscom AFB, MA 01731-5000

GL/LW
Hanscom AFB, MA 01731-5000

DARPA/PM
1400 Wilson Boulevard
Arlington, VA 22209

Defense Technical
  Information Center
Cameron Station
Alexandria, VA 22314
(5 copies)

Defense Intelligence Agency
Directorate for Scientific &
  Technical Intelligence
Washington, D.C. 20301

Defense Nuclear Agency/SPSS
ATTN: Dr. Michael Shore
6801 Telegraph Road
Alexandria, VA 22310

AFTAC/CA (STINFO)
Patrick AFB, FL 32925-6001

Dr. Gregory van der Vink
Congress of the United States
Office of Technology Assessment
Washington, D.C. 20510

Mr. Alfred Lieberman
ACDA/VI-OA'State Department Building
Room 5726
320 - 21St Street, NW
Washington, D.C. 20451

TACTEC
Battelle Memorial Institute
505 King Avenue
Columbus, OH 43201 (Final report only)